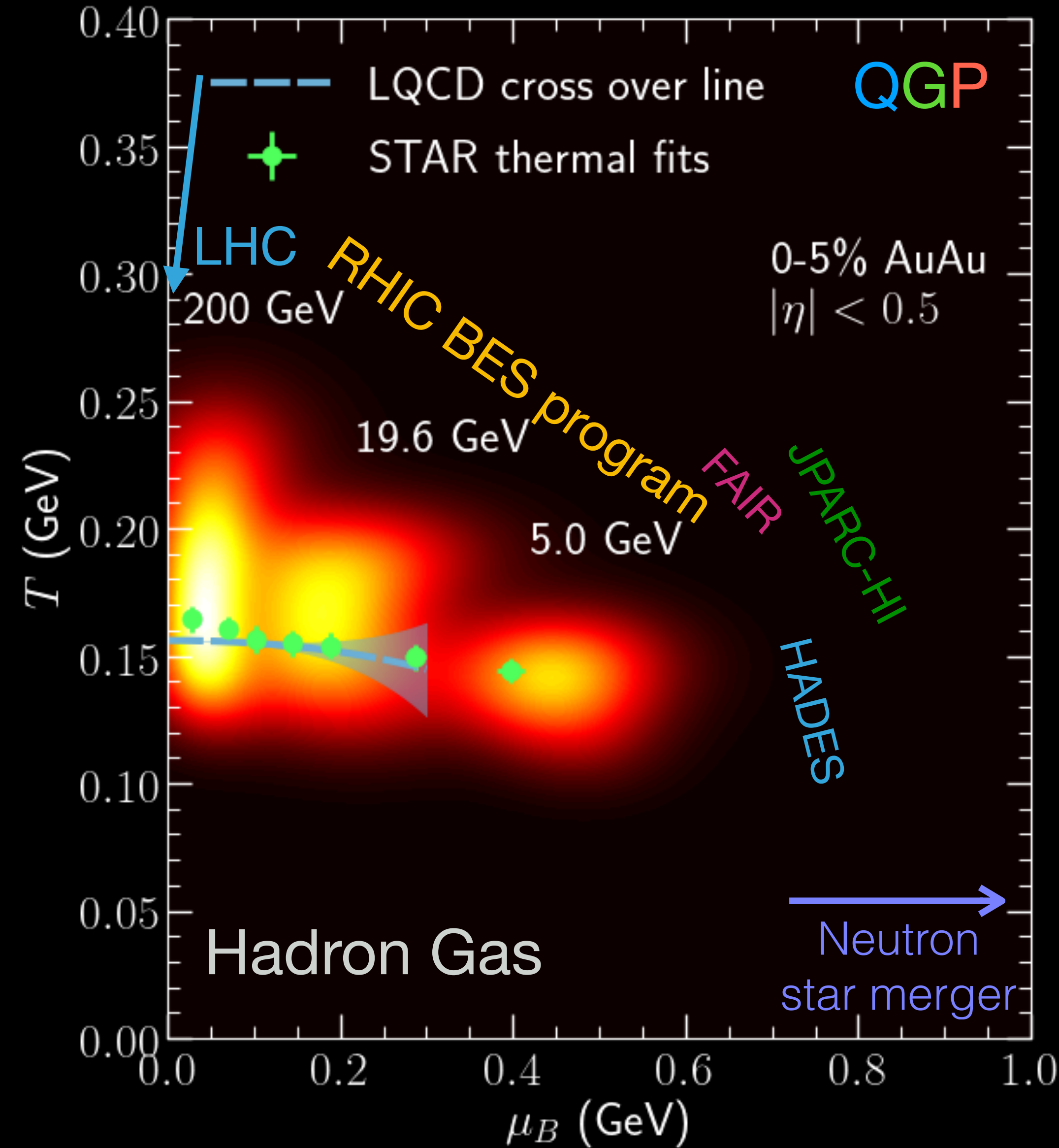
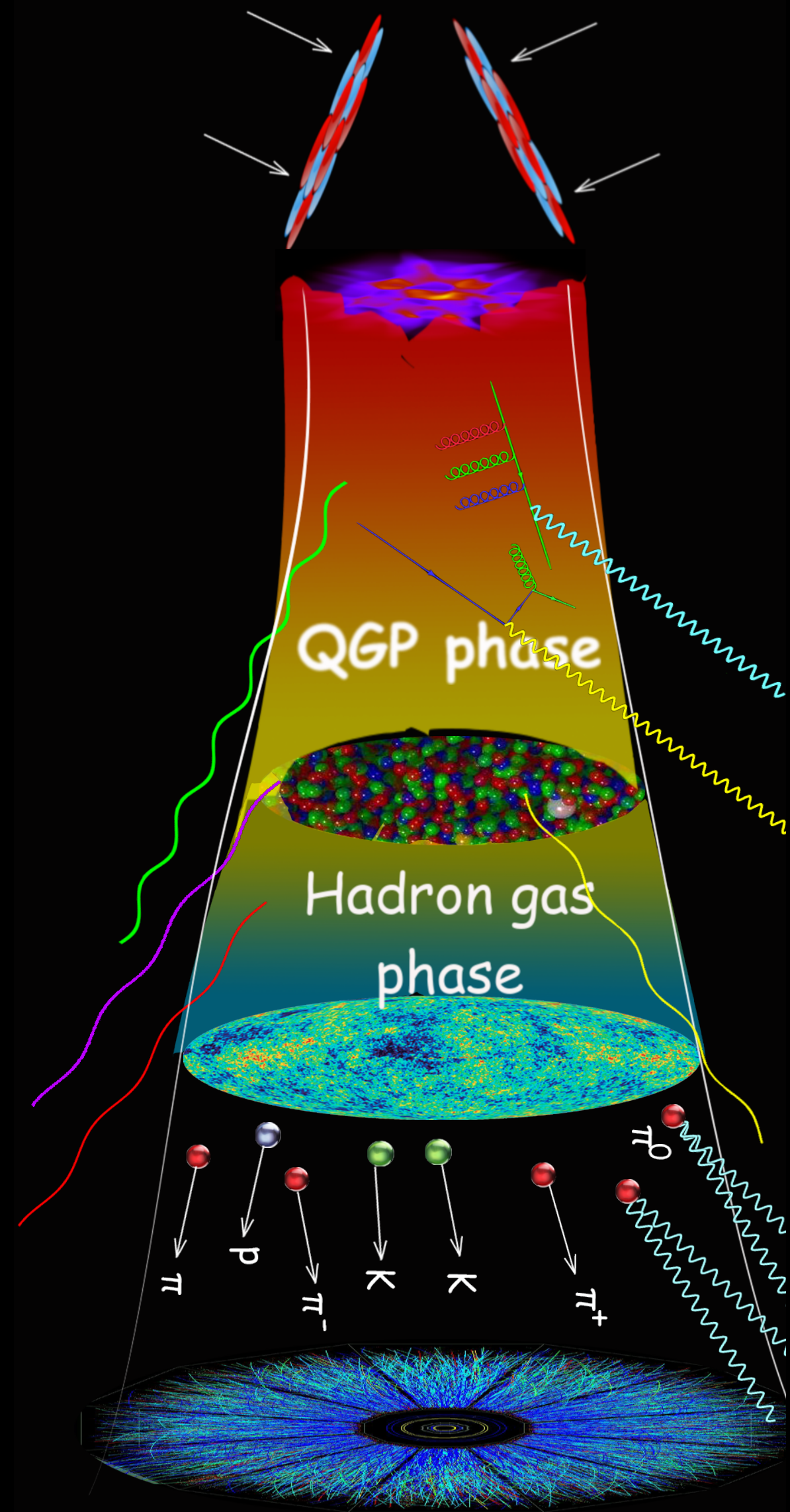


Bayesian Inference of QGP Properties and 3D Dynamics from Beam Energy Scan Data

Chun Shen (Wayne State University)

In collaboration with Björn Schenke and Wenbin Zhao

PROBING THE NUCLEAR MATTER PHASE DIAGRAM



- Search for a critical point & 1st order phase transition

$$c_s^2(T, \{\mu_q\})$$

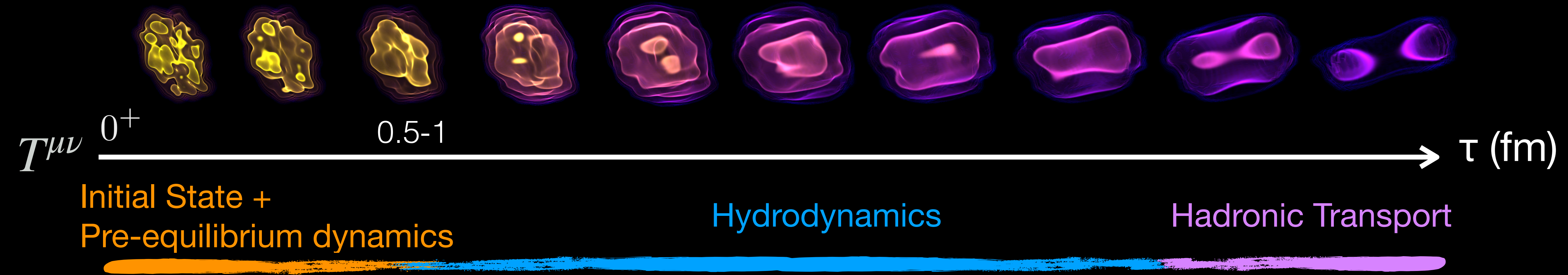
- How do the QGP transport properties change with baryon doping?

$$(\eta/s)(T, \{\mu_q\}), (\zeta/s)(T, \{\mu_q\})$$

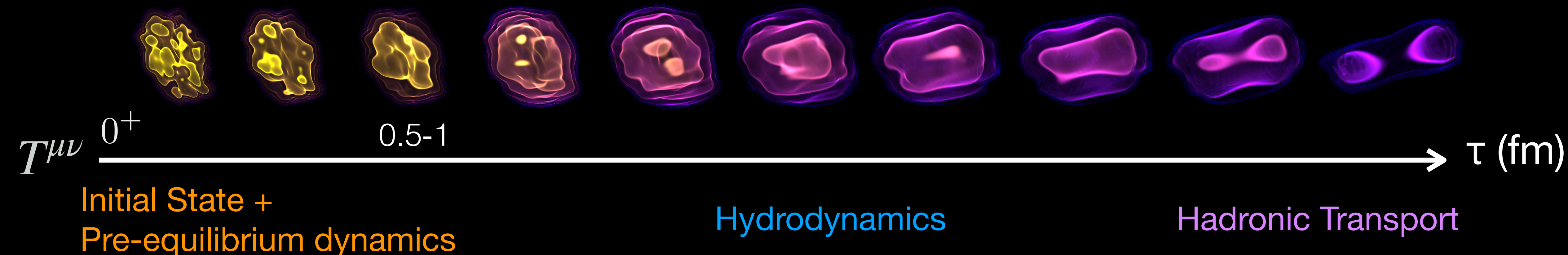
- Access to new transport phenomena

Charge diffusion

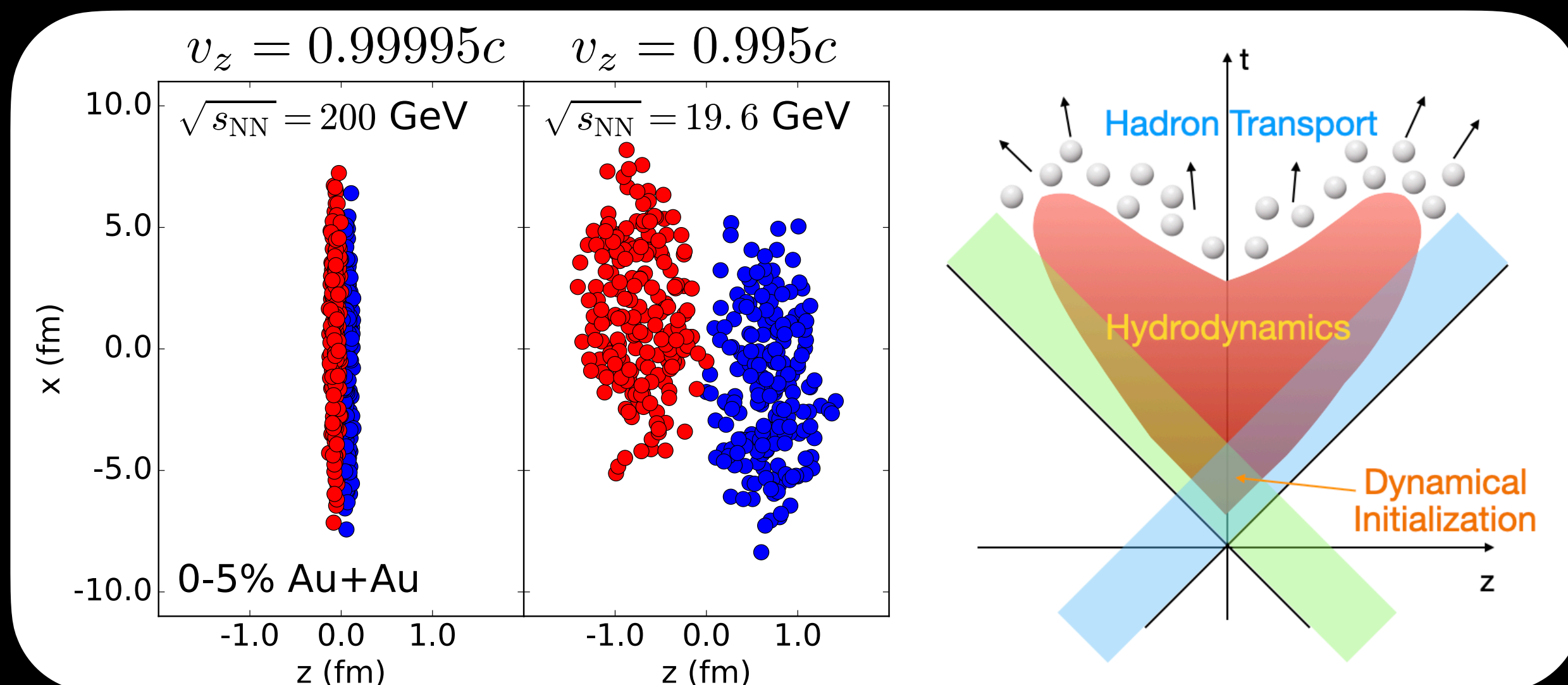
THE MULTI-STAGE THEORETICAL FRAMEWORK



THE MULTI-STAGE THEORETICAL FRAMEWORK



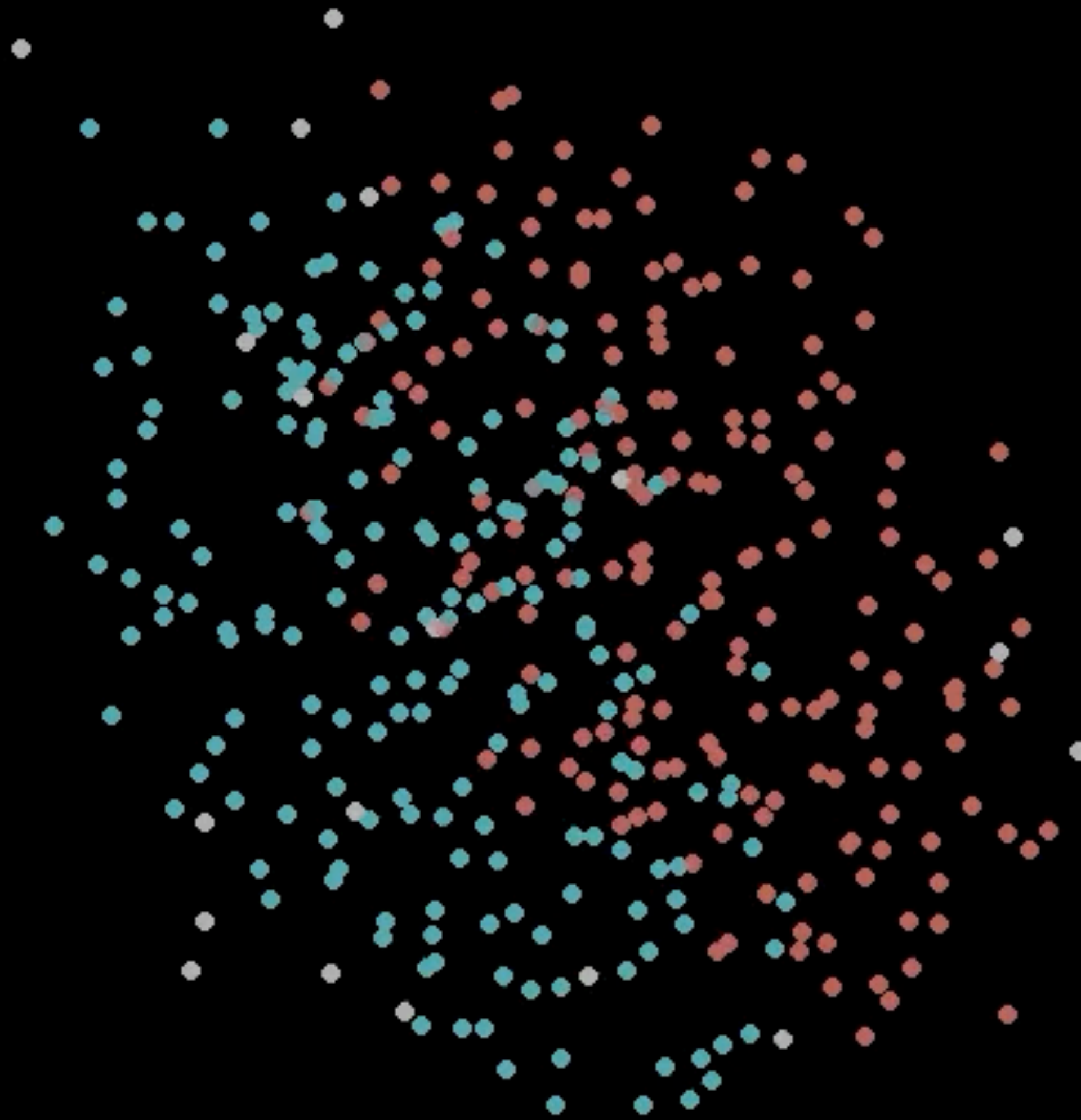
RHIC BES energies



$$\partial_\mu T^{\mu\nu} = J^\nu_{\text{source}}$$

$$\partial_\mu J^\mu = \rho_{\text{source}}$$

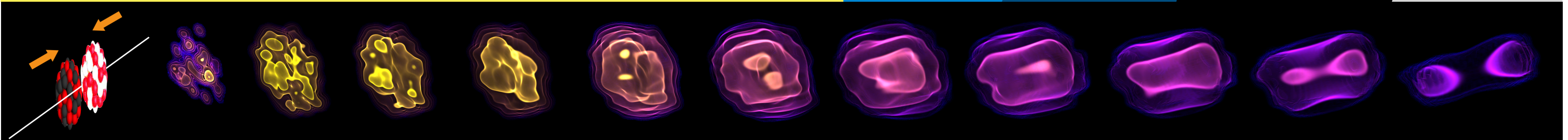
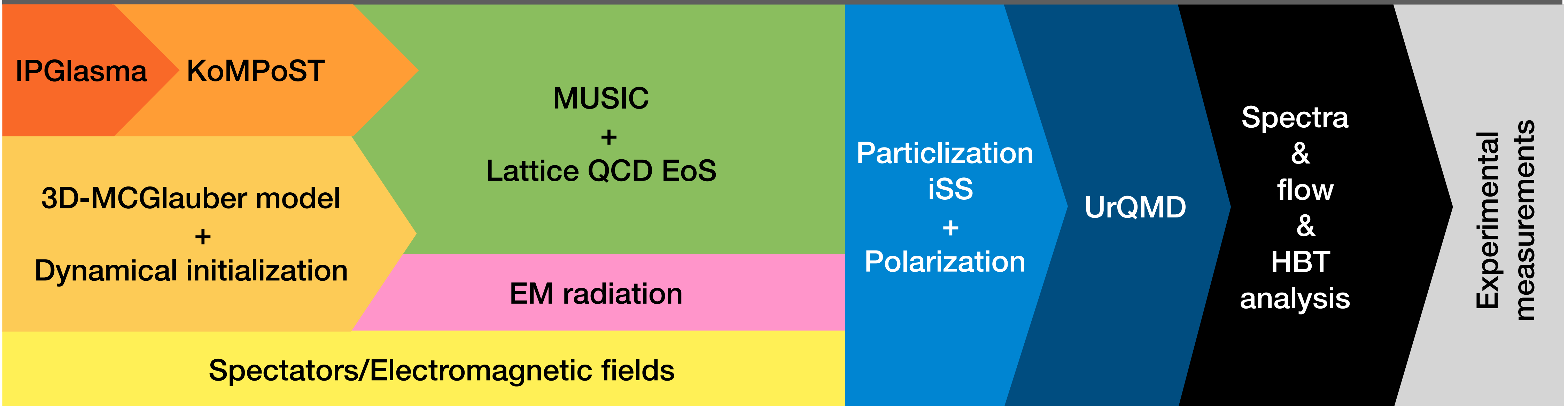
0-5% Au+Au @ 19.6 GeV



AN OPEN SOURCE HYBRID FRAMEWORK—IEBE-MUSIC

 <https://github.com/chunshen1987/iEBE-MUSIC>

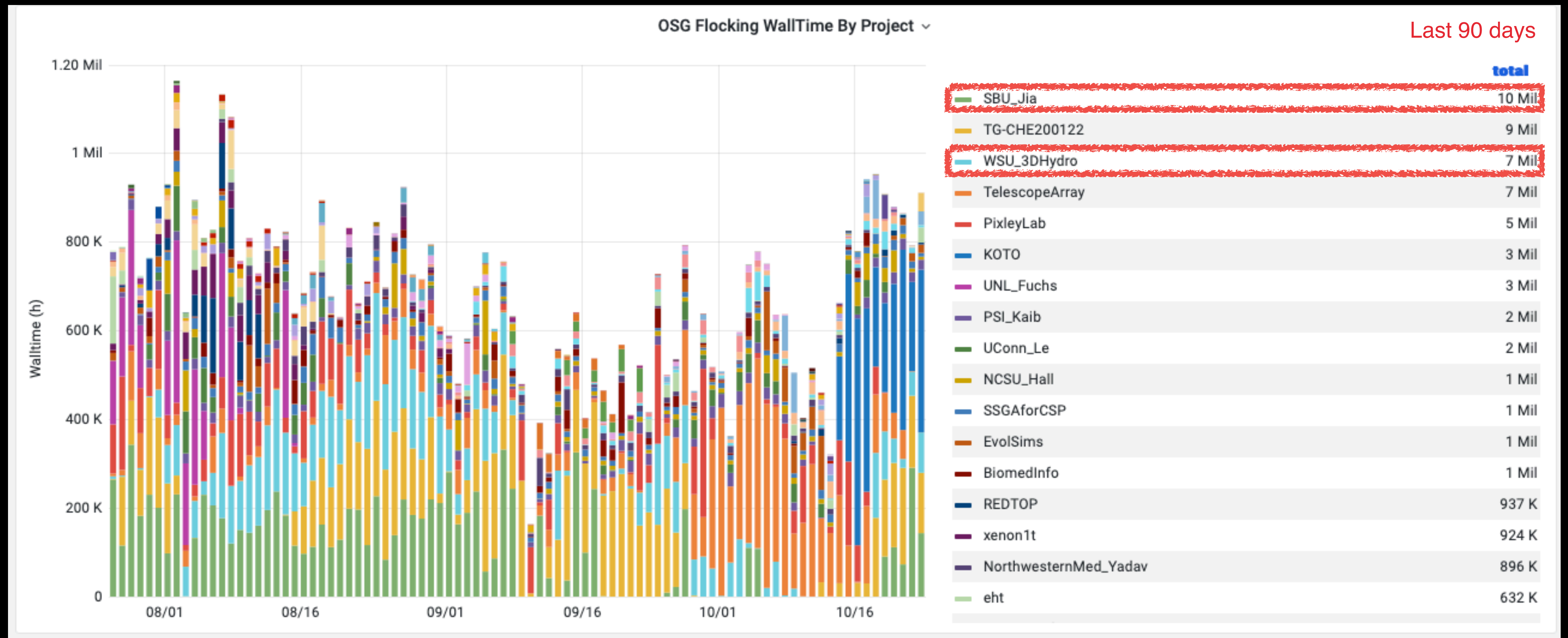
The iEBE-MUSIC Framework



State-of-the-art event-by-event simulations for relativistic heavy-ion collisions

AN OPEN SOURCE FRAMEWORK FOR THE COMMUNITY

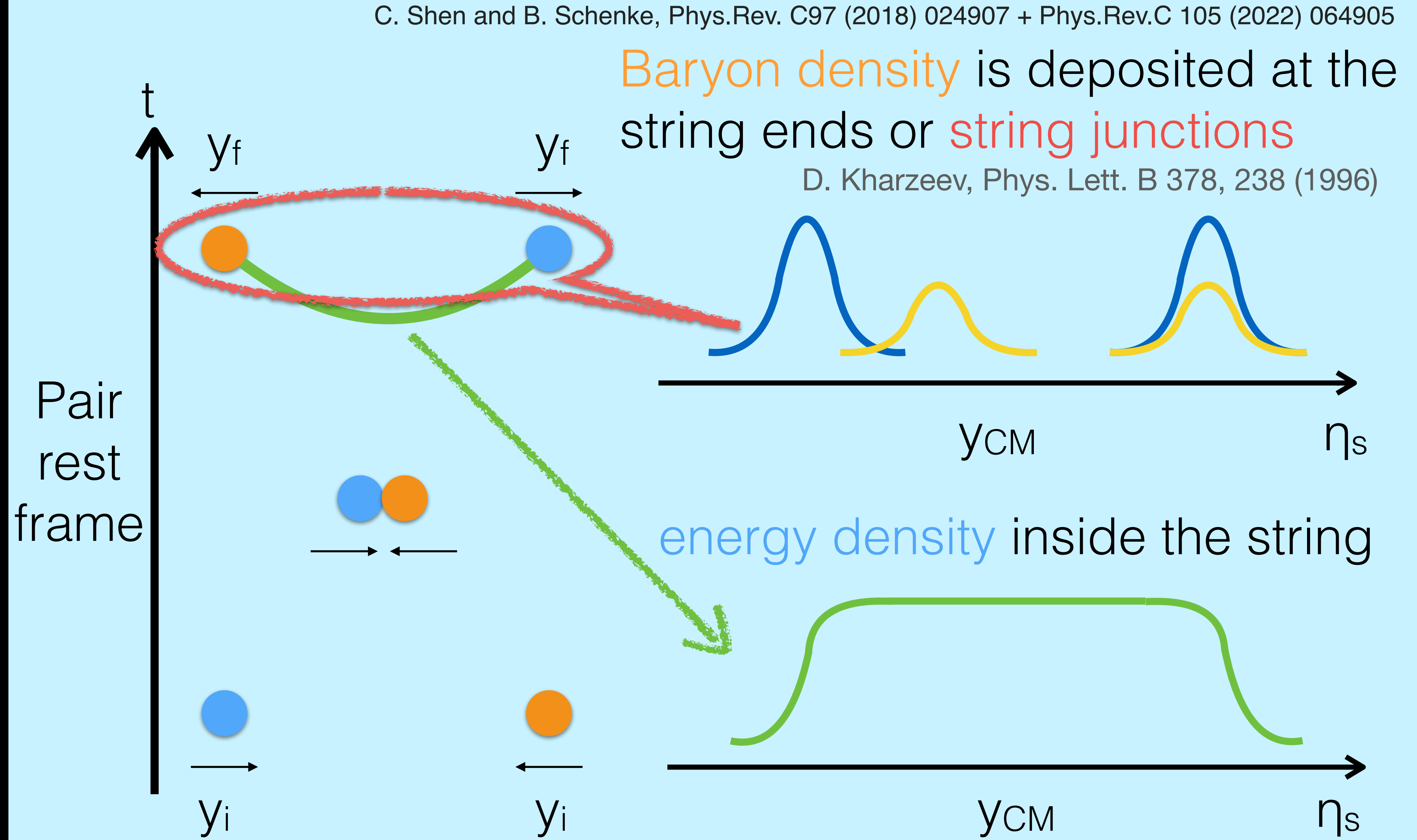
The iEBE-MUSIC framework takes advantage of **free** computing resources powered by the Open Science Grid (OSG) 



3D MC-GLAUBER MODEL WITH STRING DECELERATION

C. Shen and B. Schenke, Phys.Rev. C97 (2018) 024907 + Phys.Rev.C 105 (2022) 064905

Baryon density is deposited at the string ends or string junctions
D. Kharzeev, Phys. Lett. B 378, 238 (1996)



- Transverse collision geometry is determined by MC-Glauber model

- 3 valence quarks are sampled from PDF with

$$\sum_i x_i \leq 1$$

- Incoming quarks are decelerated with a string tension σ ,

$$dp^z/dt = -\sigma$$

Imposed conservation for energy, momentum, and net baryon density

3D MC-GLAUBER MODEL WITH STRING DECELERATION

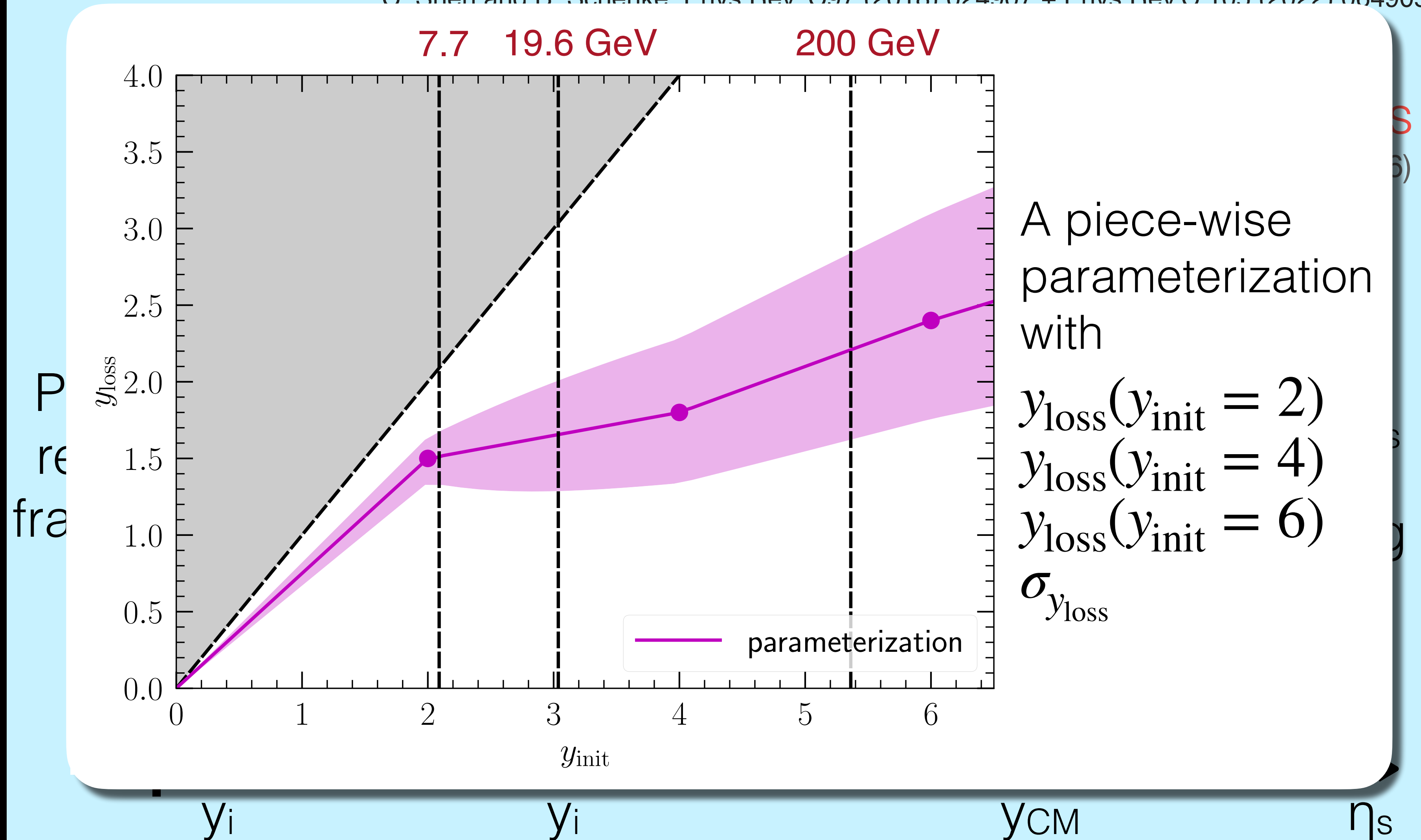
C. Shen and B. Schenke, Phys Rev C 97 (2018) 024907 + Phys Rev C 105 (2022) 064905

- Transverse collision geometry is determined by MC-Glauber model
- 3 valence quarks are sampled from PDF with

$$\sum_i x_i \leq 1$$

- Incoming quarks are decelerated with a string tension σ ,

$$dp^z/dt = -\sigma$$



Imposed conservation for energy, momentum, and net baryon density

QCD EQUATION OF STATE AT FINITE DENSITIES

M. Albright, J. Kapusta and C. Young, Phys. Rev. C90, 024915 (2014)

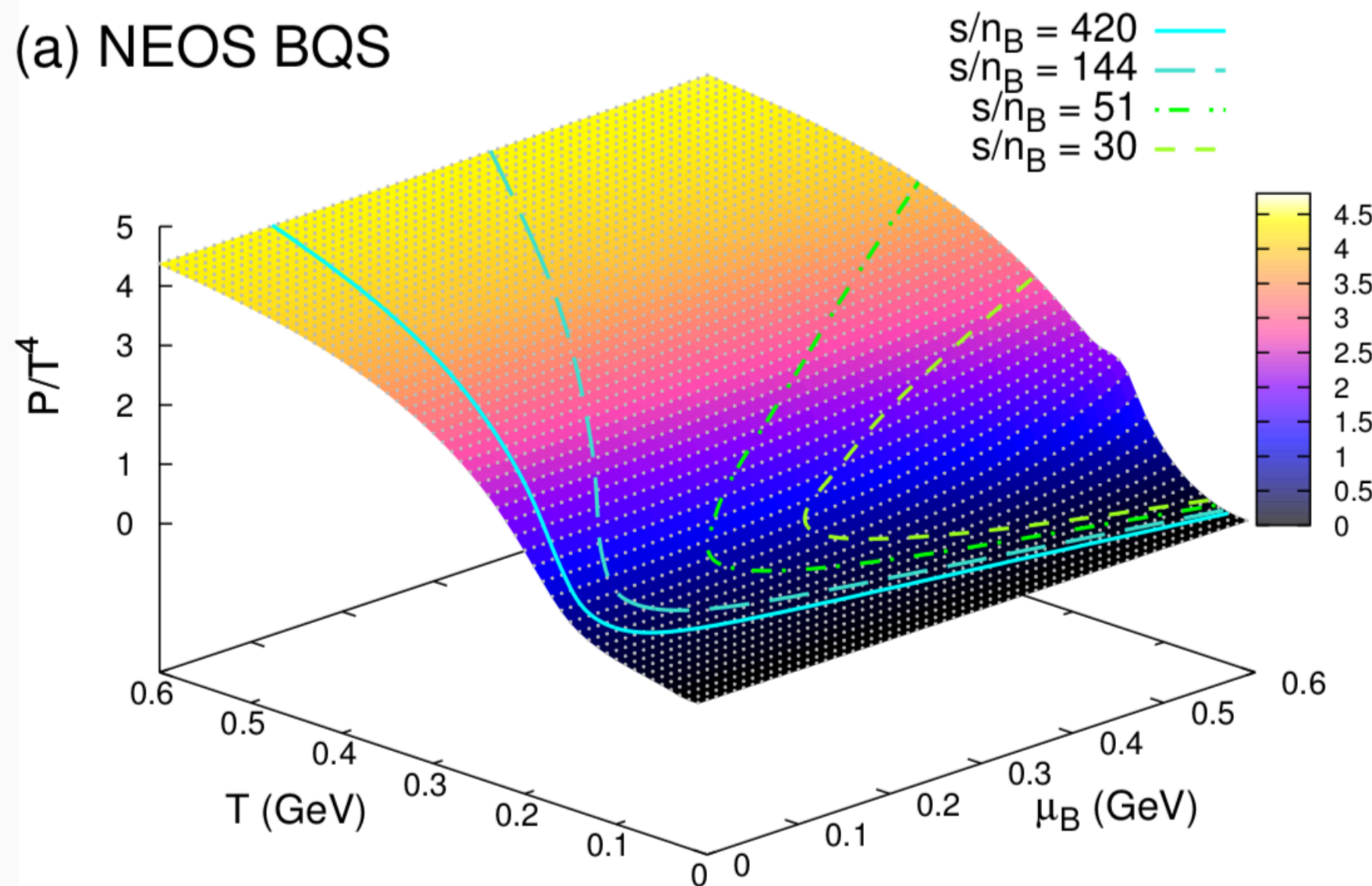
A. Monnai, B. Schenke and C. Shen, Phys. Rev. C100, 024907 (2019)

J. Noronha-Hostler, P. Parotto, C. Ratti and J. M. Stafford, Phys. Rev. C100, 064910 (2019)

J. M. Stafford *et. al*, arXiv:2103.08146 [hep-ph]

$$n_s = 0 \quad n_Q = 0.4n_B$$

(a) NEOS BQS



Lattice QCD: Taylor expansion up to the 4th order

$$\frac{P}{T^4} = \frac{P_0}{T^4} + \sum_{l,m,n} \frac{\chi_{l,m,n}^{B,Q,S}}{l!m!n!} \left(\frac{\mu_B}{T}\right)^l \left(\frac{\mu_Q}{T}\right)^m \left(\frac{\mu_S}{T}\right)^n$$

Match to Hadron Resonance Gas model at low T

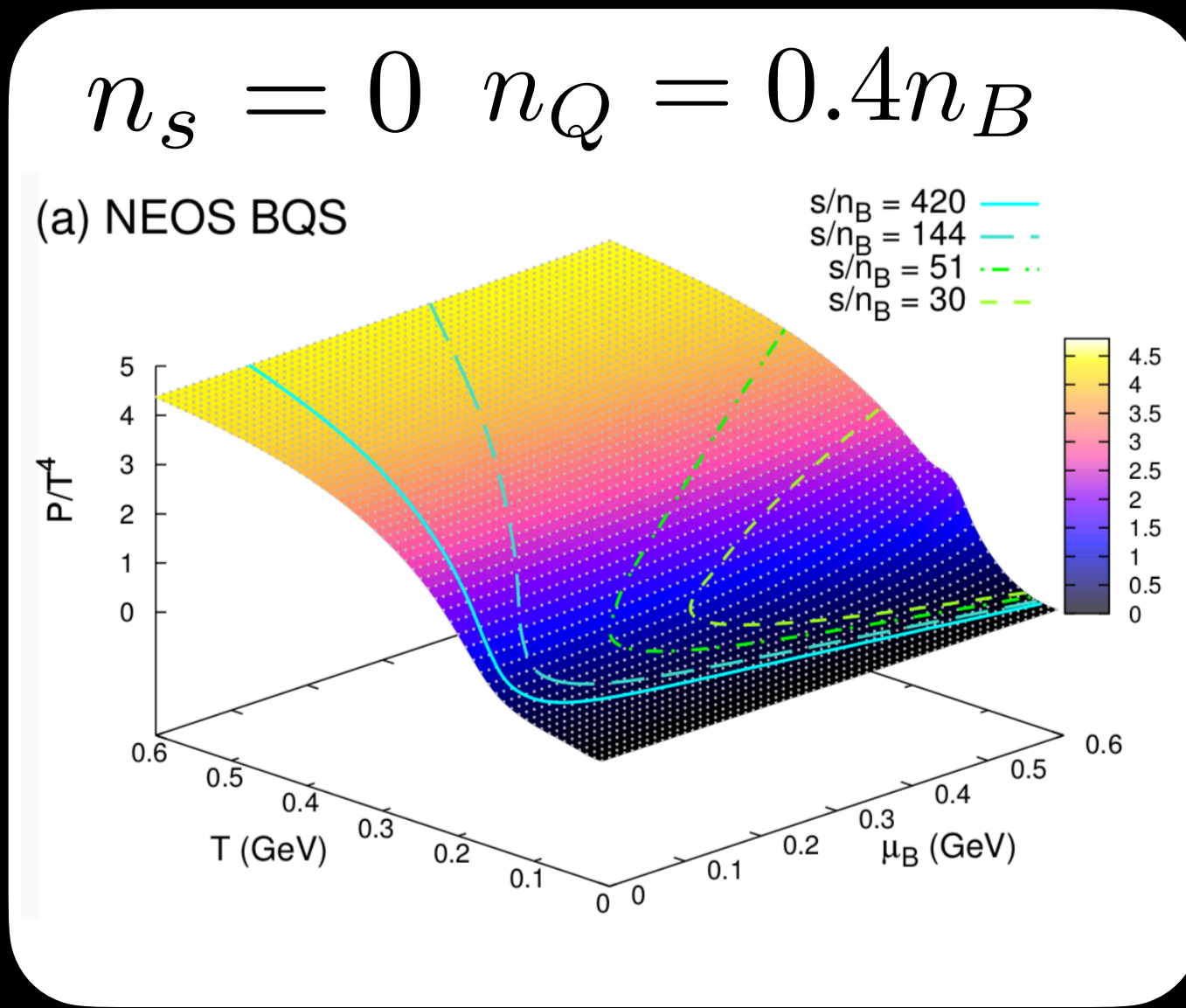
$$\frac{P}{T^4} = \frac{1}{2} [1 - f(T, \mu_B)] \frac{P_{\text{had}}(T, \mu_B)}{T^4} + \frac{1}{2} [1 + f(T, \mu_B)] \frac{P_{\text{lat}}(T, \mu_B)}{T^4}$$

$$f(T, \mu_B) = \tanh[(T - T_c(\mu_B))/\Delta T_c]$$

Enabled hydrodynamic simulations at finite μ

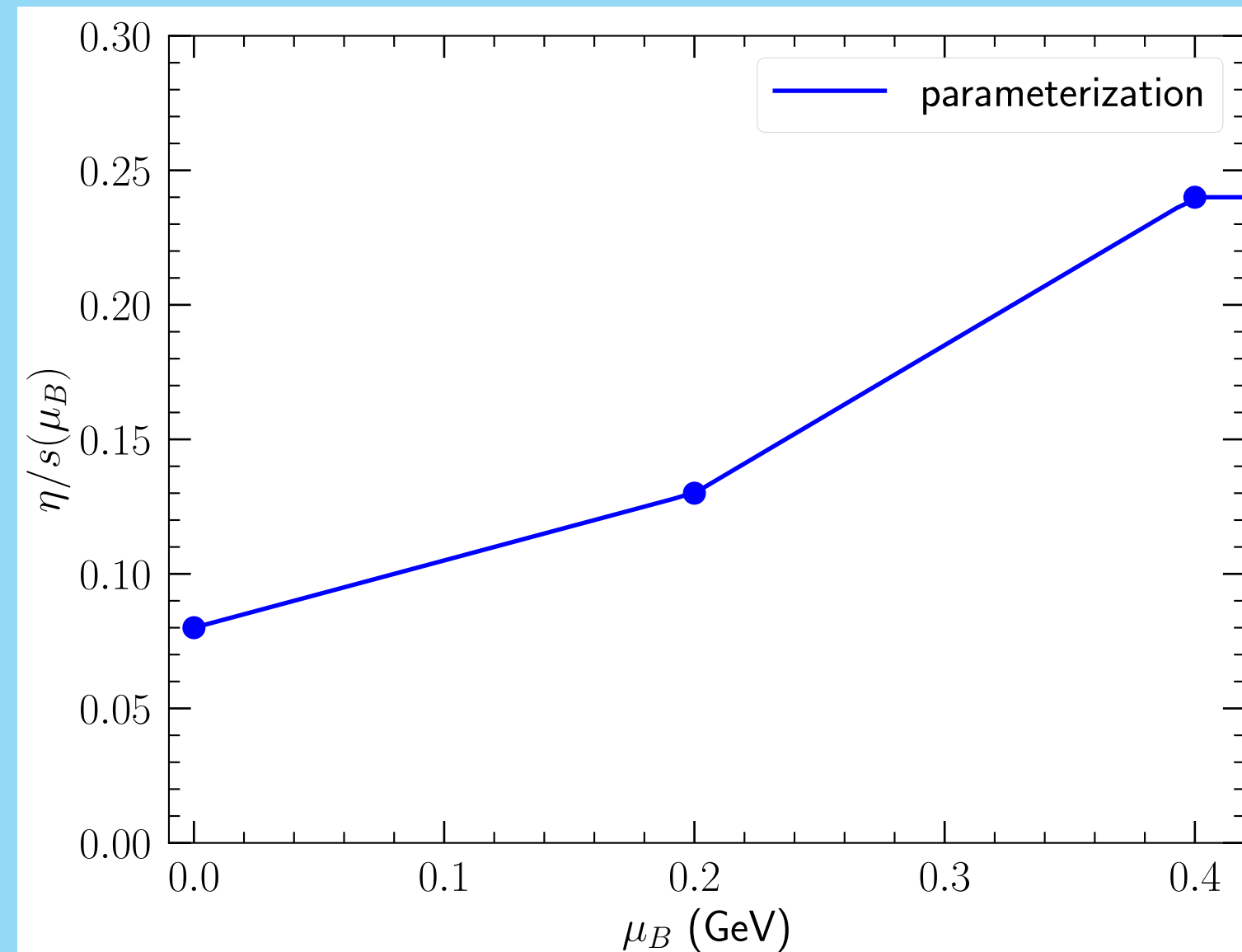
3D HYDRODYNAMICS WITH FINITE BARYON CURRENT

$$\partial_\mu T^{\mu\nu} = J^\nu_{\text{source}} + \partial_\mu J^\mu = \rho_{\text{source}}$$

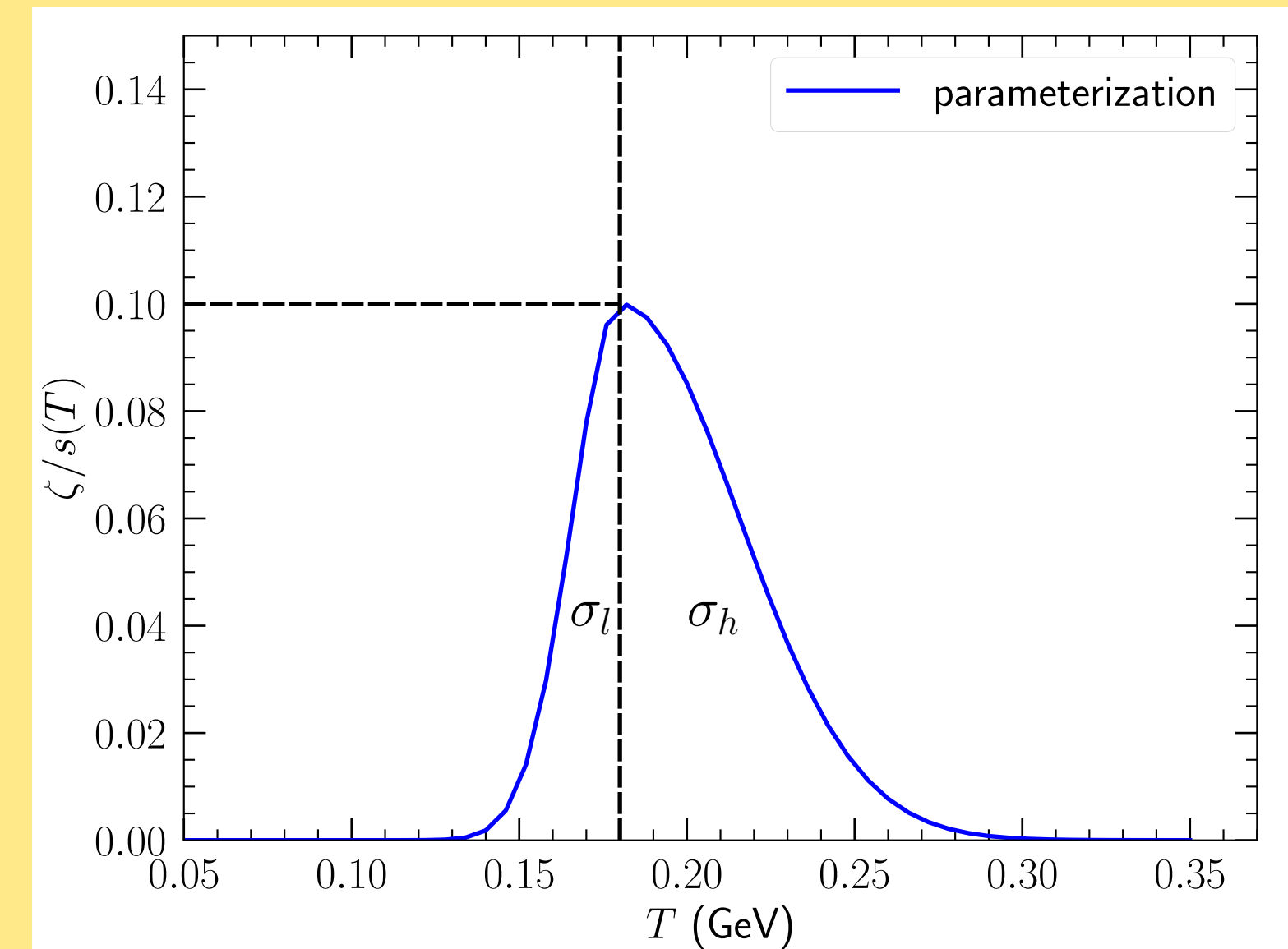


A. Monnai, B. Schenke and C. Shen, Phys. Rev. C100, 024907 (2019)

$\eta/s(\mu_B)$ has a piece-wise parameterization



$\zeta/s(T)$ is parameterized with an asymmetric Gaussian



THE MODEL PARAMETERS

TABLE I. The 20 model parameters and their prior ranges.

Parameter	Prior	Parameter	Prior
B_G (GeV^{-2})	[1, 25]	$\alpha_{\text{string tilt}}$	[0, 1]
$\alpha_{\text{shadowing}}$	[0, 1]	α_{preFlow}	[0, 2]
$y_{\text{loss},2}$	[0, 2]	η_0	[0.001, 0.3]
$y_{\text{loss},4}$	[1, 3]	η_2	[0.001, 0.3]
$y_{\text{loss},6}$	[1, 4]	η_4	[0.001, 0.3]
$\sigma_{y_{\text{loss}}}$	[0.1, 0.8]	ζ_{max}	[0, 0.2]
α_{Rem}	[0, 1]	$T_{\zeta,0}$ (GeV)	[0.15, 0.25]
λ_B	[0, 1]	$\sigma_{\zeta,+}$ (GeV)	[0.01, 0.15]
σ_x^{string} (fm)	[0.1, 0.8]	$\sigma_{\zeta,-}$ (GeV)	[0.005, 0.1]
$\sigma_\eta^{\text{string}}$	[0.1, 1]	e_{sw} (GeV/fm^3)	[0.15, 0.5]

MODEL TRAINING & OBSERVABLE SELECTION

A 20-dimensional model parameter space with 1,000 training points

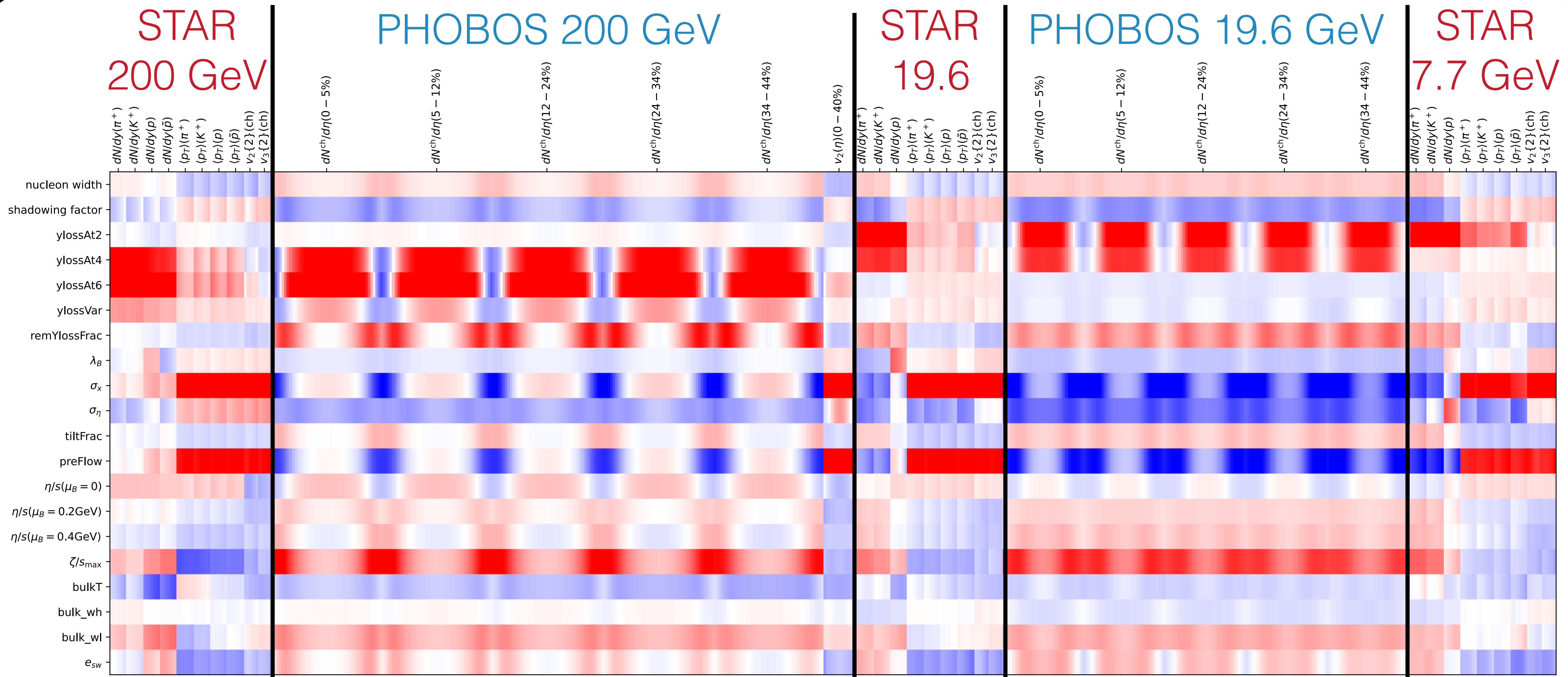
Au+Au	Hydro events per design	Avg. hadronic events per hydro
200 GeV	1,000	1,000
19.6 GeV	2,000	4,000
7.7 GeV	2,000	8,000

604 experimental data points

Au+Au	STAR midrapidity data vs. centrality	PHOBOS rapidity distribution
200 GeV	$dN/dy(\pi^+, K^+, p, \bar{p})$ $\langle p_T \rangle(\pi^+, K^+, p, \bar{p})$ $v_2^{\text{ch}}\{2\}, v_3^{\text{ch}}\{2\}$	$dN^{\text{ch}}/d\eta$ $v_2(\eta)$
19.6 GeV	$dN/dy(\pi^+, K^+, p)$ $\langle p_T \rangle(\pi^+, K^+, p, \bar{p})$ $v_2^{\text{ch}}\{2\}, v_3^{\text{ch}}\{2\}$	$dN^{\text{ch}}/d\eta$
7.7 GeV	$dN/dy(\pi^+, K^+, p)$ $\langle p_T \rangle(\pi^+, K^+, p, \bar{p})$ $v_2^{\text{ch}}\{2\}, v_3^{\text{ch}}\{2\}$	

Open Science Grid delivered 5 million CPU hours for the data generation

OBSERVABLE RESPONSES TO MODEL PARAMETERS



Red: Positive correlation; Blue: Negative correlation

OBSERVABLE RESPONSES TO MODEL PARAMETERS

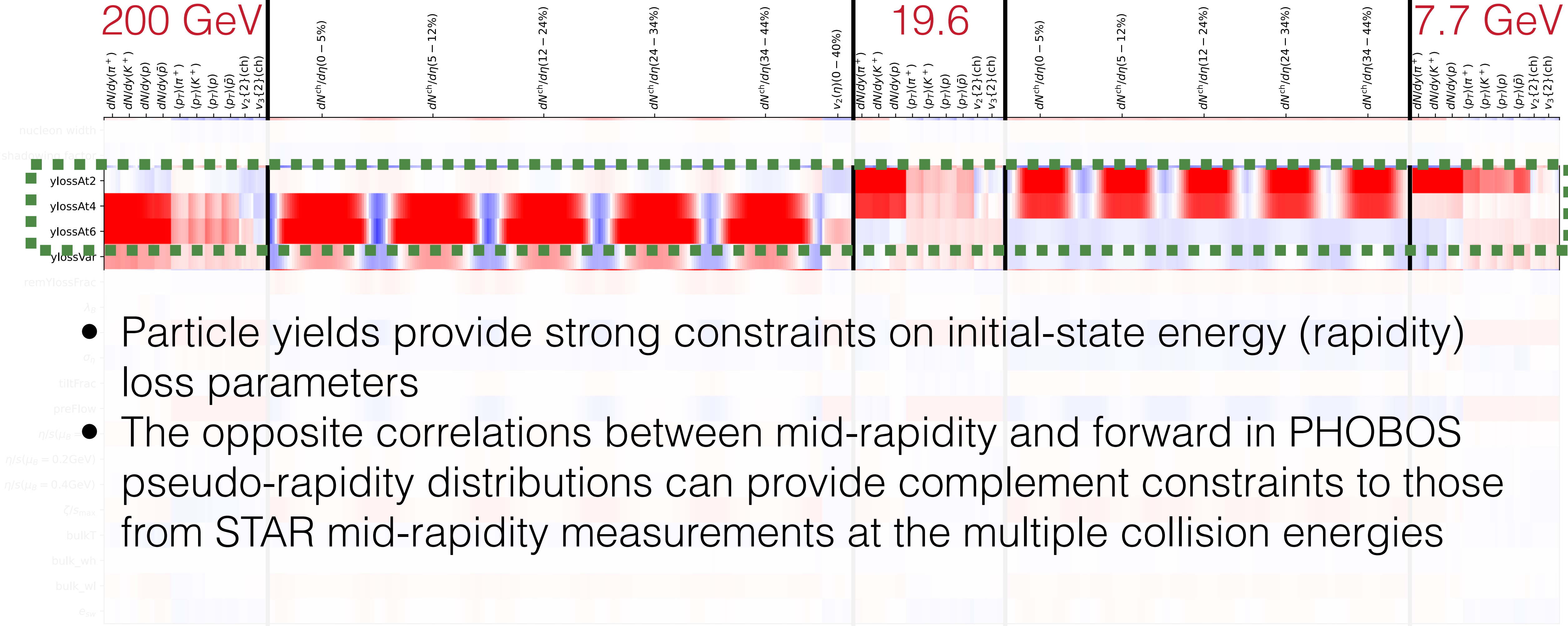
STAR
200 GeV

PHOBOS 200 GeV

STAR
19.6

PHOBOS 19.6 GeV

STAR
7.7 GeV



- Particle yields provide strong constraints on initial-state energy (rapidity) loss parameters
- The opposite correlations between mid-rapidity and forward in PHOBOS pseudo-rapidity distributions can provide complement constraints to those from STAR mid-rapidity measurements at the multiple collision energies

Red: Positive correlation; Blue: Negative correlation

OBSERVABLE RESPONSES TO MODEL PARAMETERS

STAR
200 GeV

$dN/dy(\pi^+)$
 $dN/dy(K^+)$
 $dN/dy(p)$
 $dN/dy(\bar{p})$
 $\langle p_T \rangle(\pi^+)$
 $\langle p_T \rangle(K^+)$
 $\langle p_T \rangle(p)$
 $\langle p_T \rangle(\bar{p})$
 $v_2\{2\}(ch)$
 $v_3\{2\}(ch)$

PHOBOS 200 GeV

$dN^{ch}/d\eta(0 - 5\%)$
 $dN^{ch}/d\eta(5 - 12\%)$
 $dN^{ch}/d\eta(12 - 24\%)$
 $dN^{ch}/d\eta(24 - 34\%)$
 $dN^{ch}/d\eta(34 - 44\%)$

STAR
19.6

$v_2(\eta)(0 - 40\%)$
 $dN/dy(\pi^+)$
 $dN/dy(K^+)$
 $dN/dy(p)$
 $\langle p_T \rangle(\pi^+)$
 $\langle p_T \rangle(K^+)$
 $\langle p_T \rangle(p)$
 $\langle p_T \rangle(\bar{p})$
 $v_2\{2\}(ch)$
 $v_3\{2\}(ch)$

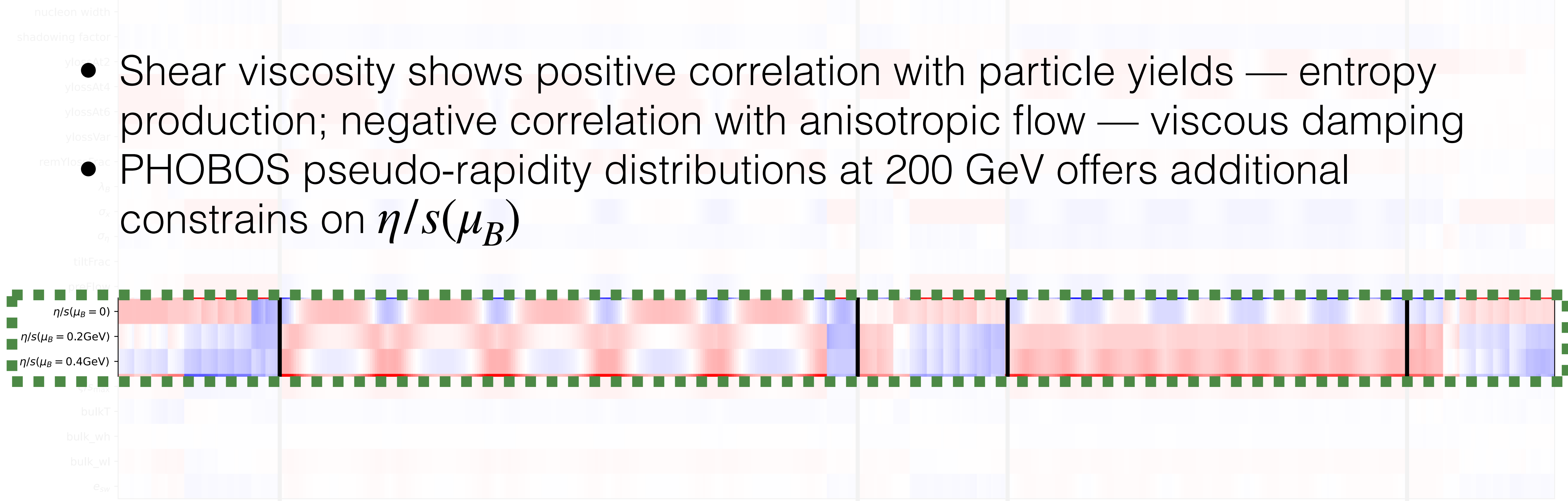
PHOBOS 19.6 GeV

$dN^{ch}/d\eta(0 - 5\%)$
 $dN^{ch}/d\eta(5 - 12\%)$
 $dN^{ch}/d\eta(12 - 24\%)$
 $dN^{ch}/d\eta(24 - 34\%)$
 $dN^{ch}/d\eta(34 - 44\%)$

STAR
7.7 GeV

$dN/dy(\pi^+)$
 $dN/dy(K^+)$
 $dN/dy(p)$
 $\langle p_T \rangle(\pi^+)$
 $\langle p_T \rangle(K^+)$
 $\langle p_T \rangle(p)$
 $\langle p_T \rangle(\bar{p})$
 $v_2\{2\}(ch)$
 $v_3\{2\}(ch)$

- Shear viscosity shows positive correlation with particle yields — entropy production; negative correlation with anisotropic flow — viscous damping
- PHOBOS pseudo-rapidity distributions at 200 GeV offers additional constrains on $\eta/s(\mu_B)$



Red: Positive correlation; Blue: Negative correlation

OBSERVABLE RESPONSES TO MODEL PARAMETERS

STAR
200 GeV

PHOBOS 200 GeV

STAR
19.6

PHOBOS 19.6 GeV

STAR
7.7 GeV

$dN/dy(\pi^+)$
 $dN/dy(K^+)$
 $dN/dy(p)$
 $dN/dy(\bar{p})$
 $\langle p_T \rangle(\pi^+)$
 $\langle p_T \rangle(K^+)$
 $\langle p_T \rangle(p)$
 $\langle p_T \rangle(\bar{p})$
 $v_2\{2\}(ch)$
 $v_3\{2\}(ch)$

$dN^{ch}/d\eta(0 - 5\%)$

$dN^{ch}/d\eta(5 - 12\%)$

$dN^{ch}/d\eta(12 - 24\%)$

$dN^{ch}/d\eta(24 - 34\%)$

$dN^{ch}/d\eta(34 - 44\%)$

$v_2(\eta)(0 - 40\%)$

$dN/dy(\pi^+)$
 $dN/dy(K^+)$
 $dN/dy(p)$
 $\langle p_T \rangle(\pi^+)$
 $\langle p_T \rangle(K^+)$
 $\langle p_T \rangle(p)$
 $\langle p_T \rangle(\bar{p})$
 $v_2\{2\}(ch)$
 $v_3\{2\}(ch)$

$dN^{ch}/d\eta(0 - 5\%)$

$dN^{ch}/d\eta(5 - 12\%)$

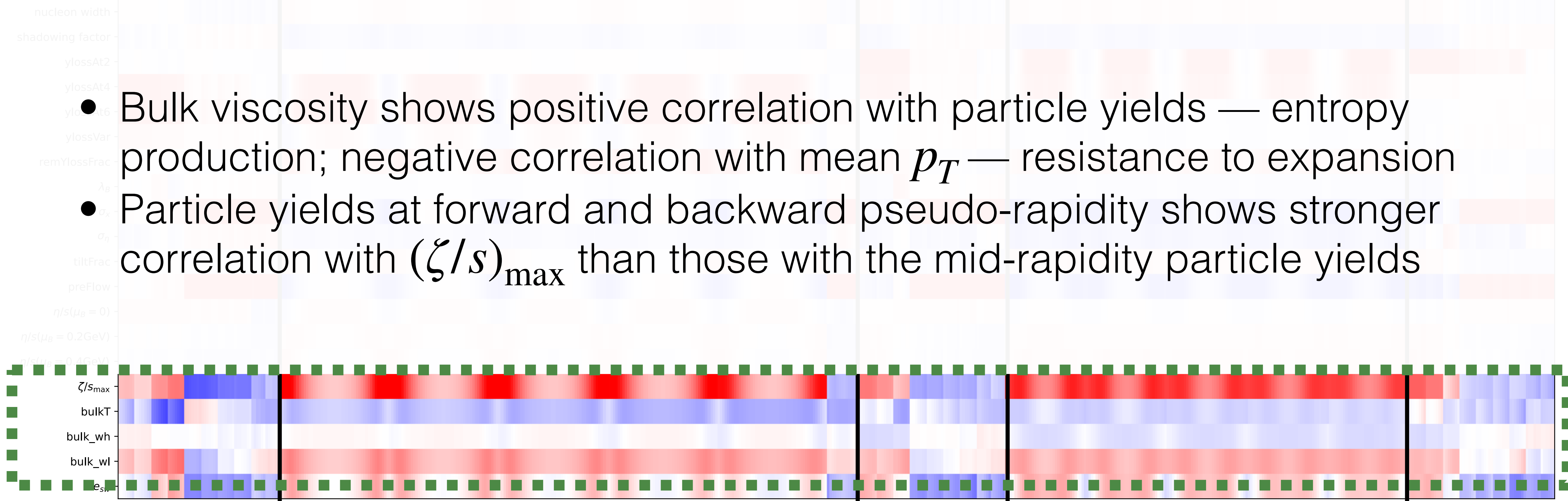
$dN^{ch}/d\eta(12 - 24\%)$

$dN^{ch}/d\eta(24 - 34\%)$

$dN^{ch}/d\eta(34 - 44\%)$

$dN/dy(\pi^+)$
 $dN/dy(K^+)$
 $dN/dy(p)$
 $\langle p_T \rangle(\pi^+)$
 $\langle p_T \rangle(K^+)$
 $\langle p_T \rangle(p)$
 $\langle p_T \rangle(\bar{p})$
 $v_2\{2\}(ch)$
 $v_3\{2\}(ch)$

- Bulk viscosity shows positive correlation with particle yields — entropy production; negative correlation with mean p_T — resistance to expansion
- Particle yields at forward and backward pseudo-rapidity shows stronger correlation with $(\zeta/s)_{\max}$ than those with the mid-rapidity particle yields



Red: Positive correlation; Blue: Negative correlation

PUBLIC INTERACTIVE MODEL EMULATOR



3D-Glauber + MUSIC + UrQMD Model for RHIC BES energies

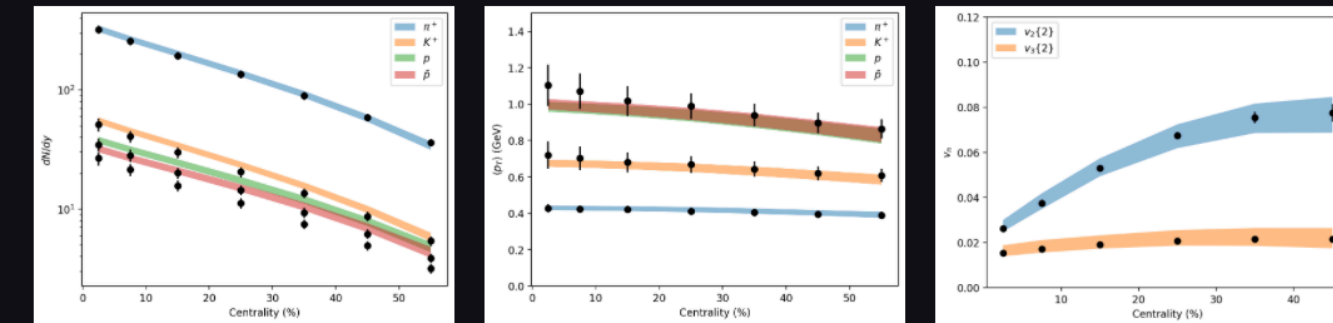
This is an interactive web page that emulates particle production and their anisotropic flow as functions of rapidity using the 3D-Glauber+MUSIC+UrQMD model.

This work is based on [link](#)

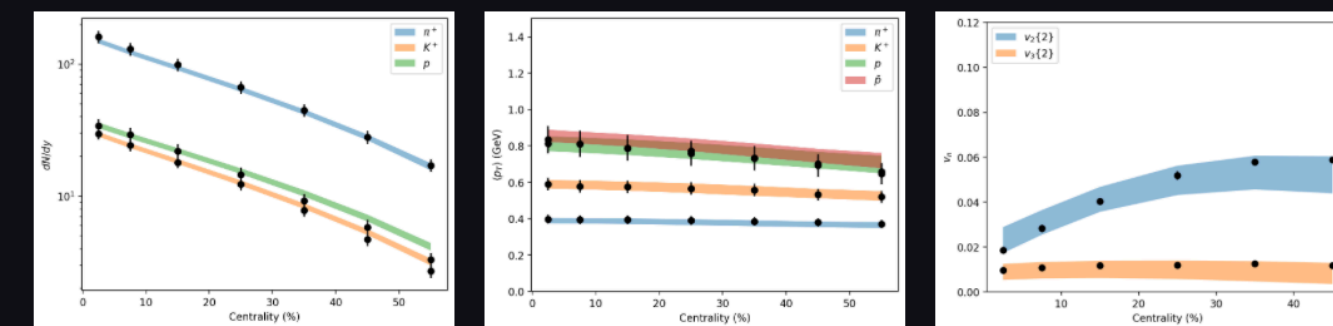
One can adjust the model parameters on the left sidebar.

The colored bands in the figure show the emulator estimations with their uncertainties. The compared experimental data are from the STAR and PHOBOS Collaborations

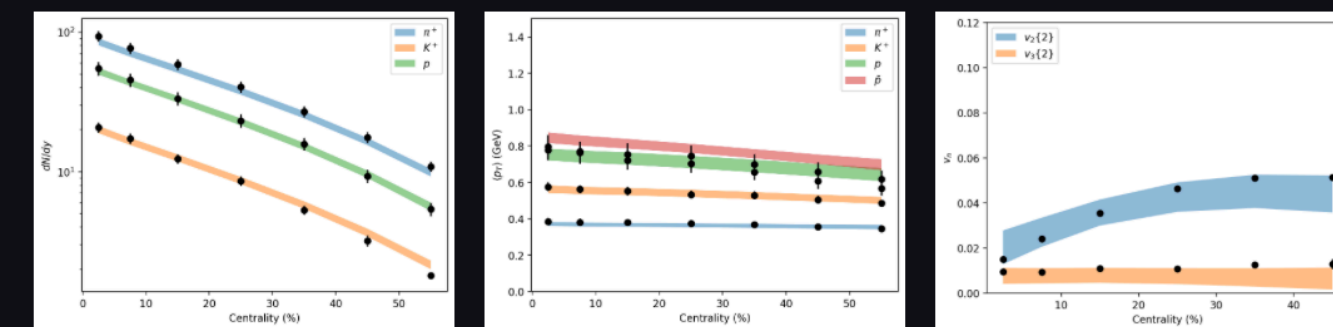
Au+Au @ 200 GeV vs. STAR



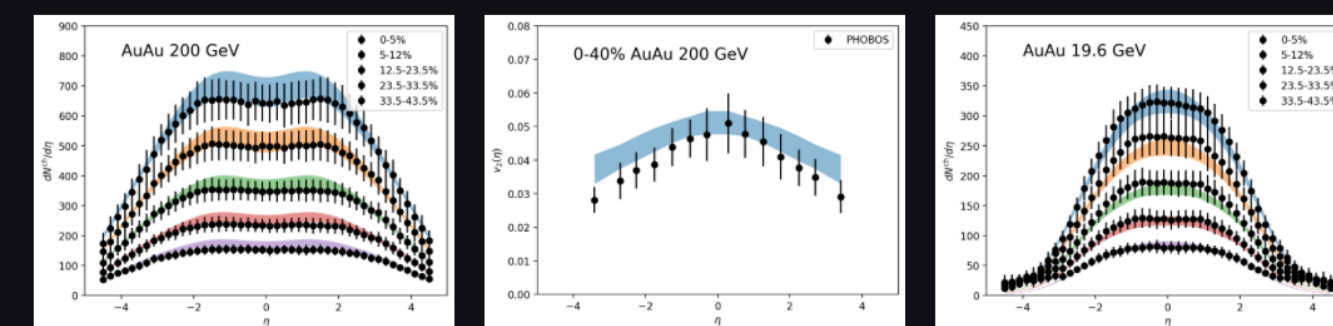
Au+Au @ 19.6 GeV vs. STAR



Au+Au @ 7.7 GeV vs. STAR



Comparisons to the PHOBOS data



[link](#)

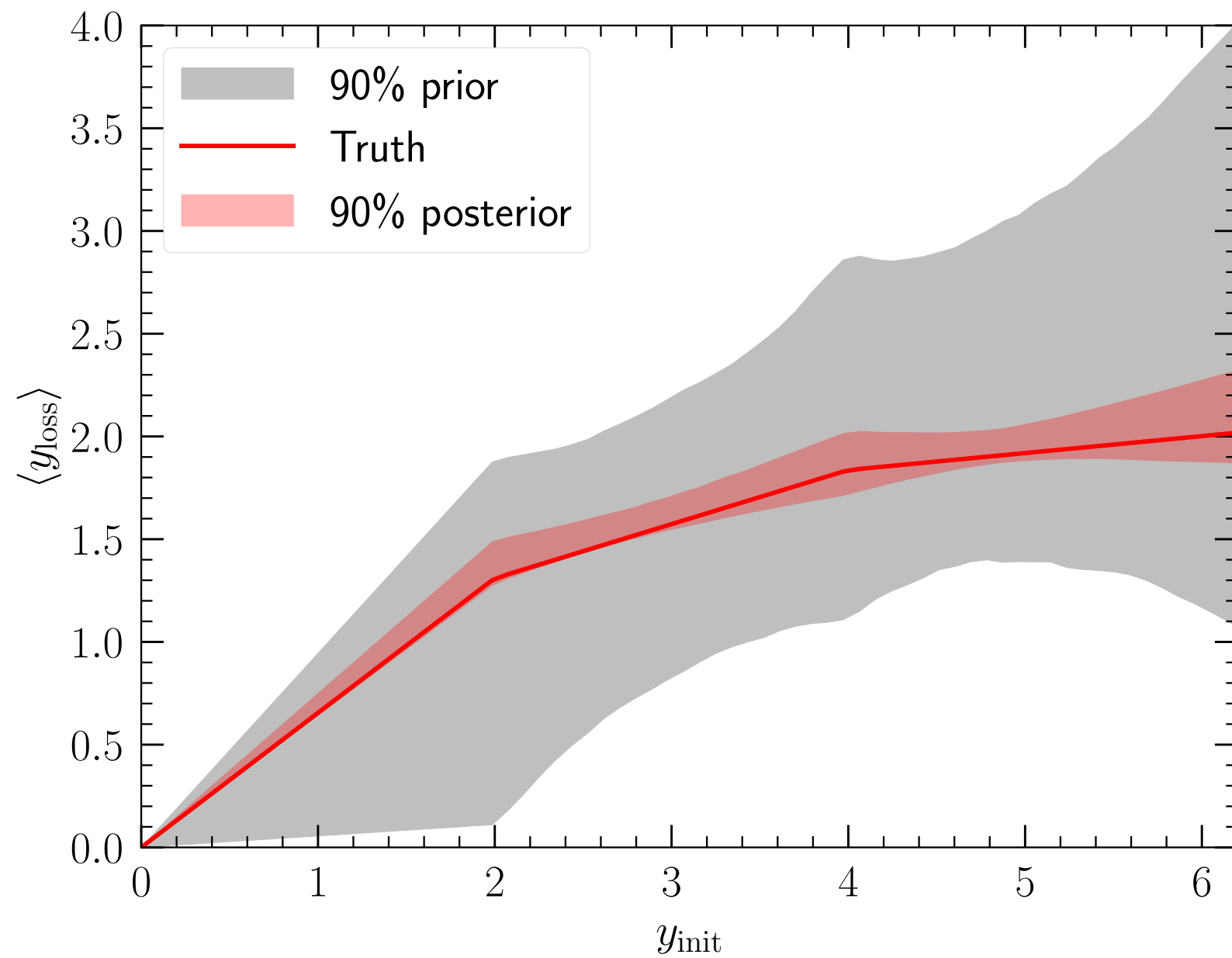


- An interactive webpage for emulating the full (3+1)D simulations for RHIC BES energies at real time
- Build your own intuition for heavy-ion phenomenology!

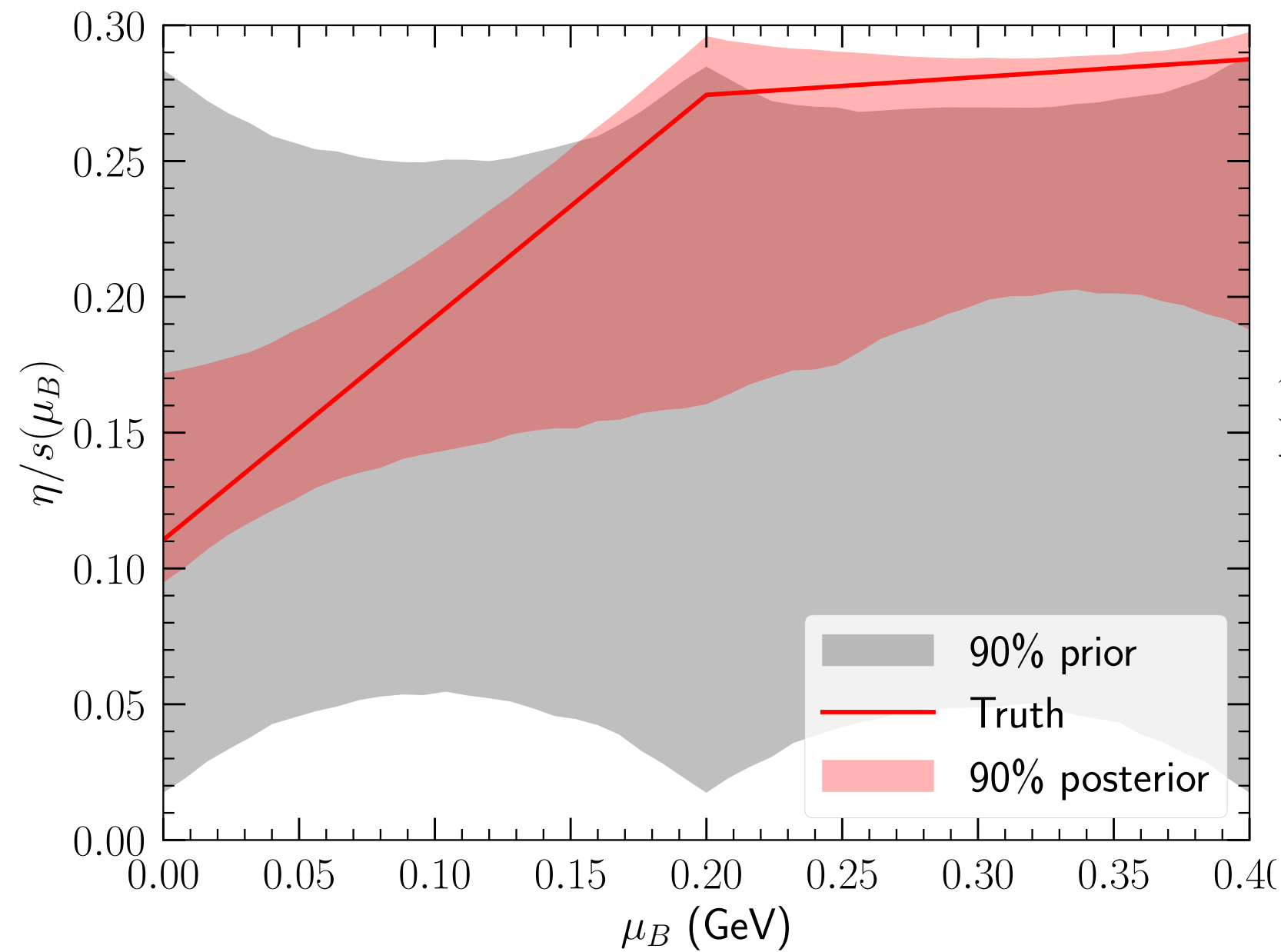
BAYESIAN VALIDATION: CLOSURE TEST

$$\text{Bayes' Theorem: } P(\theta | y_{\text{exp}}) \propto P(y_{\text{exp}} | \theta)P(\theta)$$

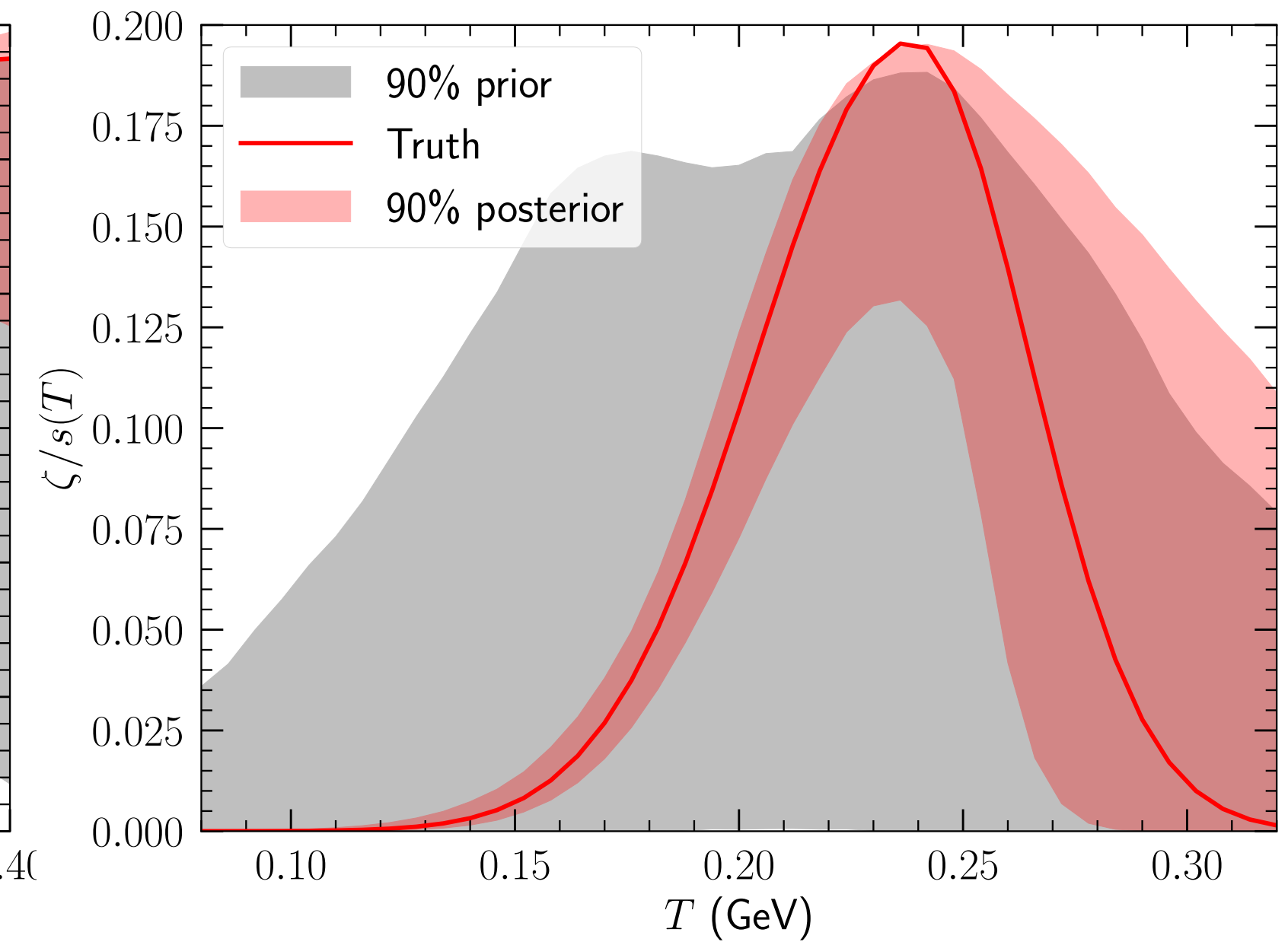
Initial-state stopping



$\eta/s(\mu_B)$



$\zeta/s(T)$



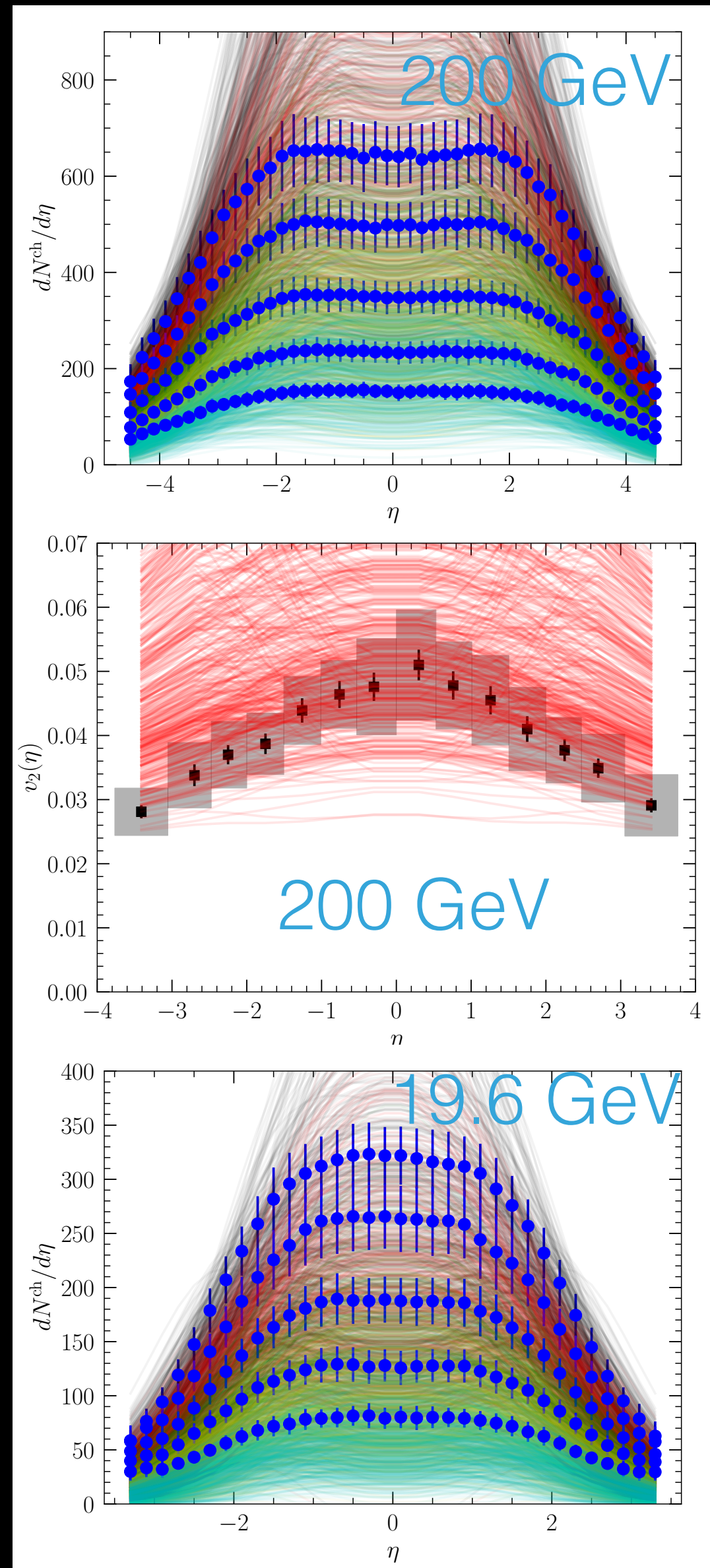
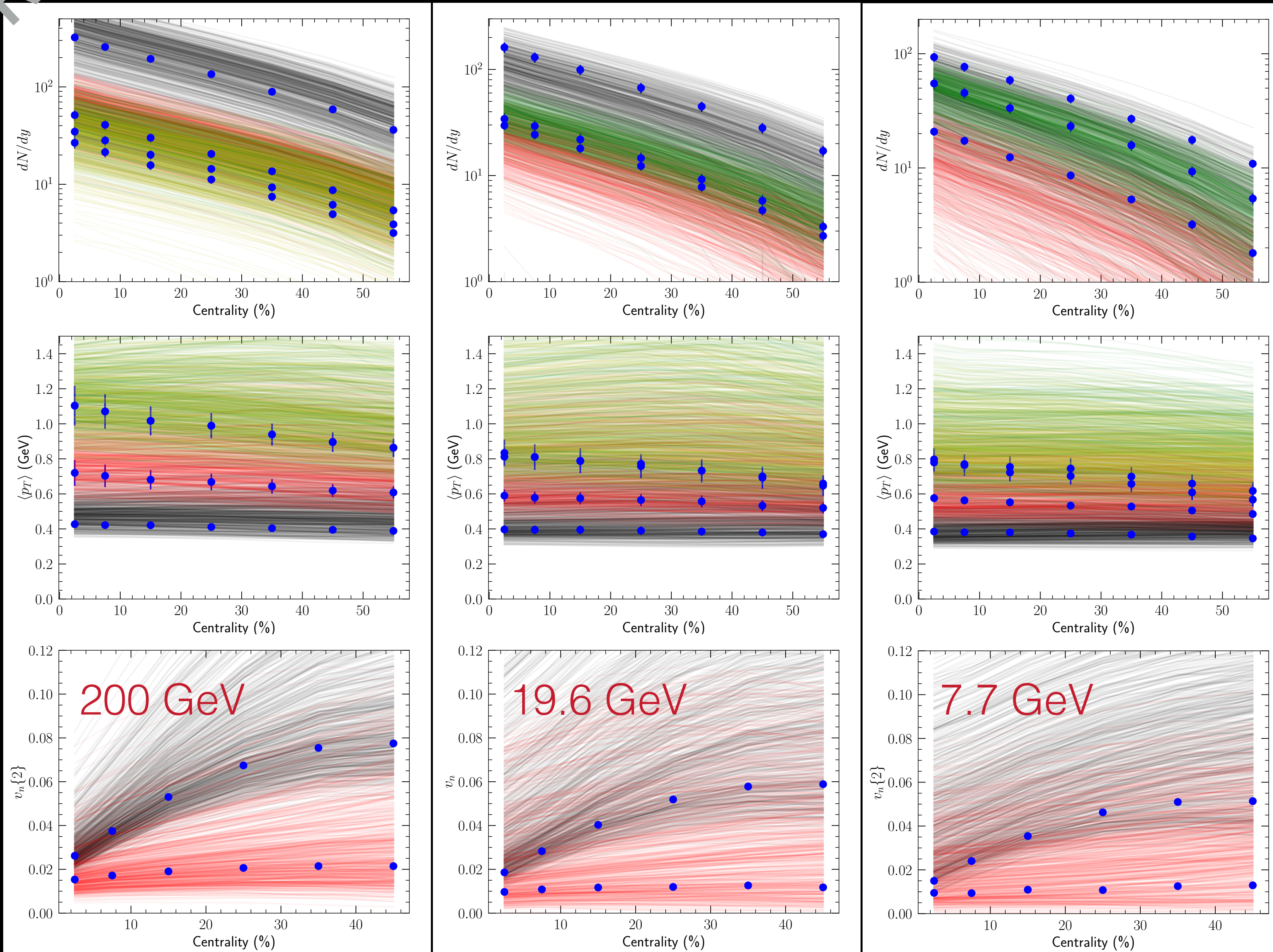
- Model emulation with Markov Chain Monte Carlo (MCMC) is verified with a closure test for initial-state stopping $y_{\text{loss}}(y_{\text{init}})$, $\eta/s(\mu_B)$, and $\zeta/s(T)$
- The selected observables can give strong constraints on the QGP properties at RHIC BES energies



BAYESIAN INFERENCE AT RHIC BES ENERGIES

PRIOR

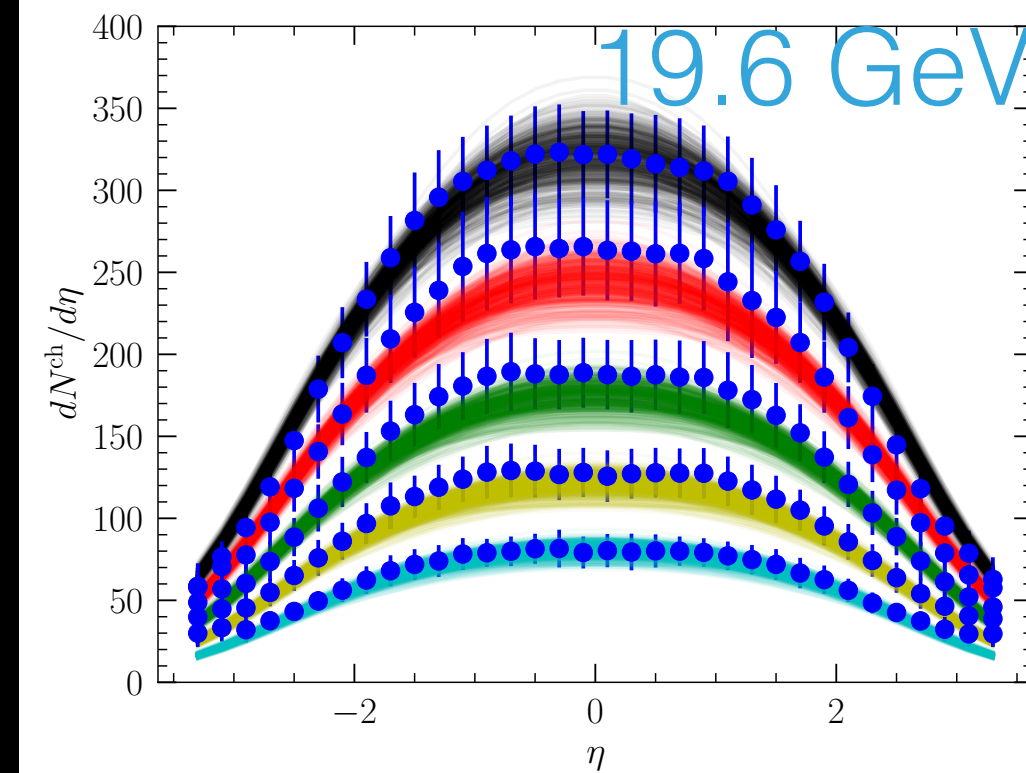
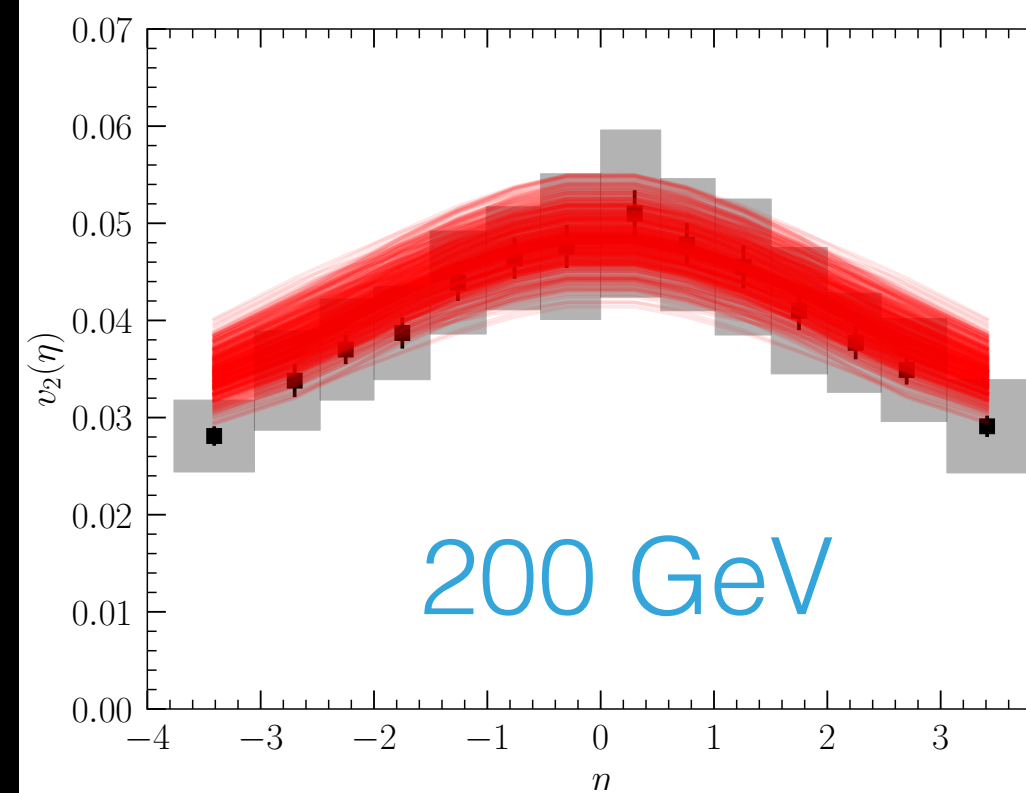
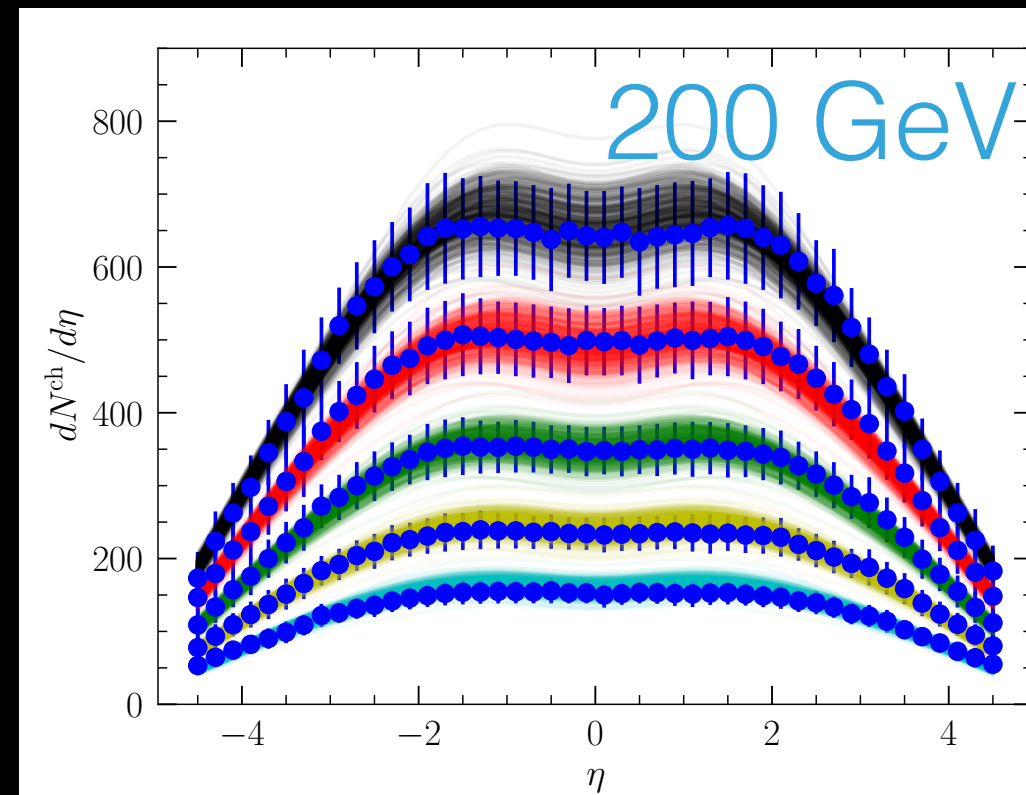
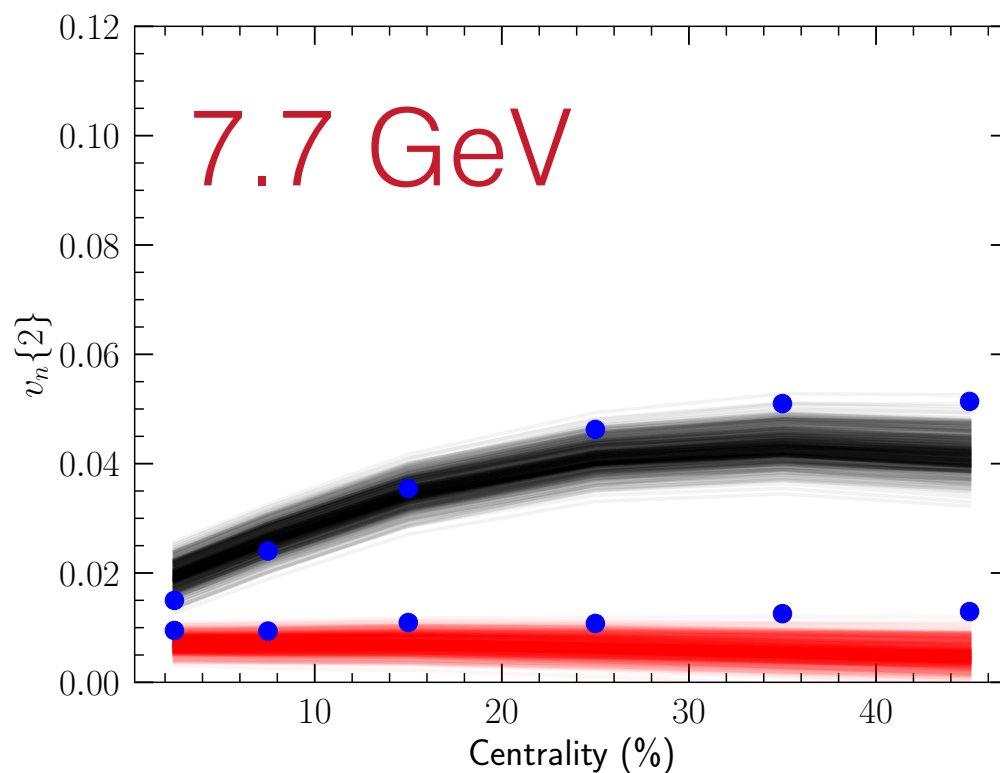
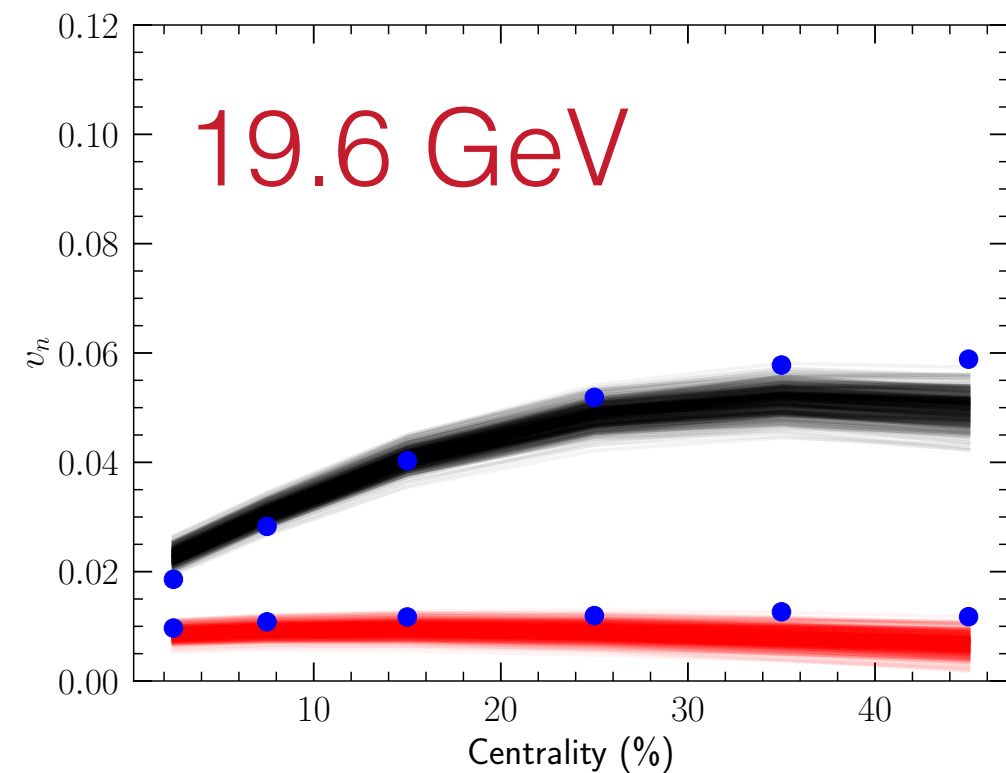
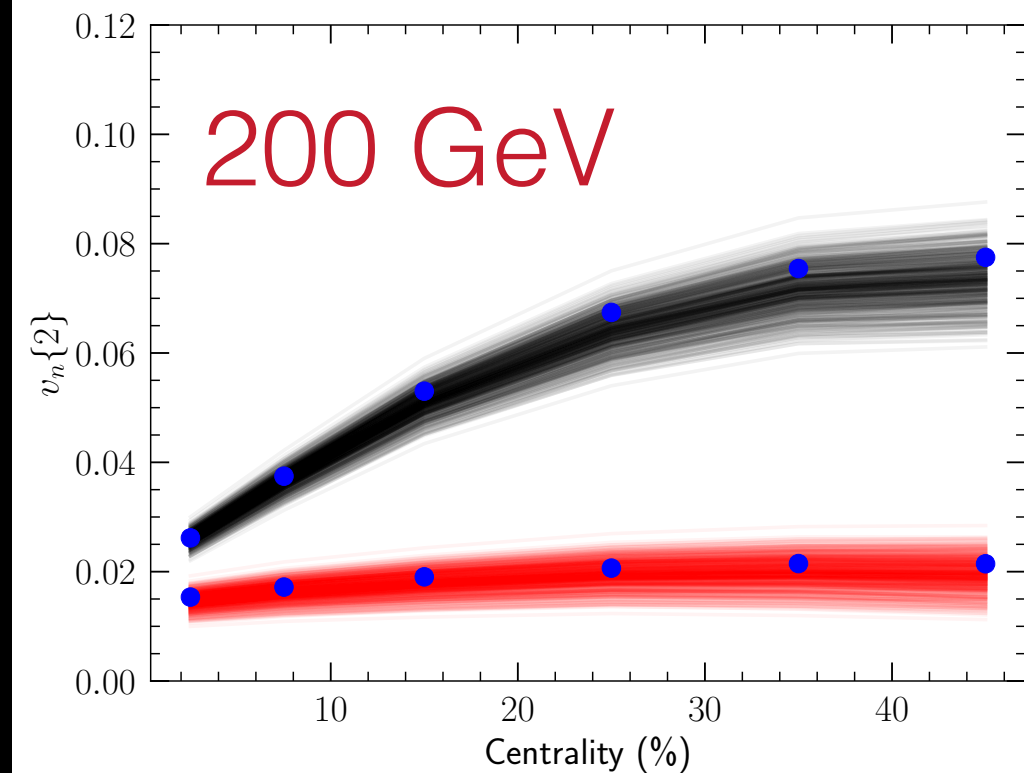
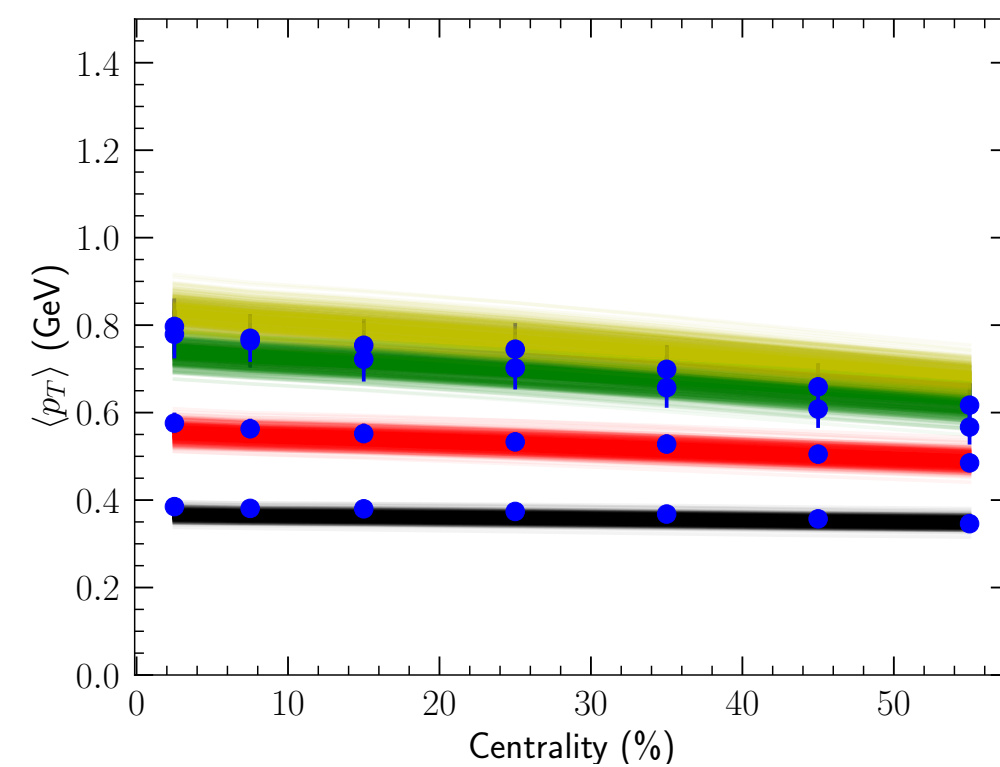
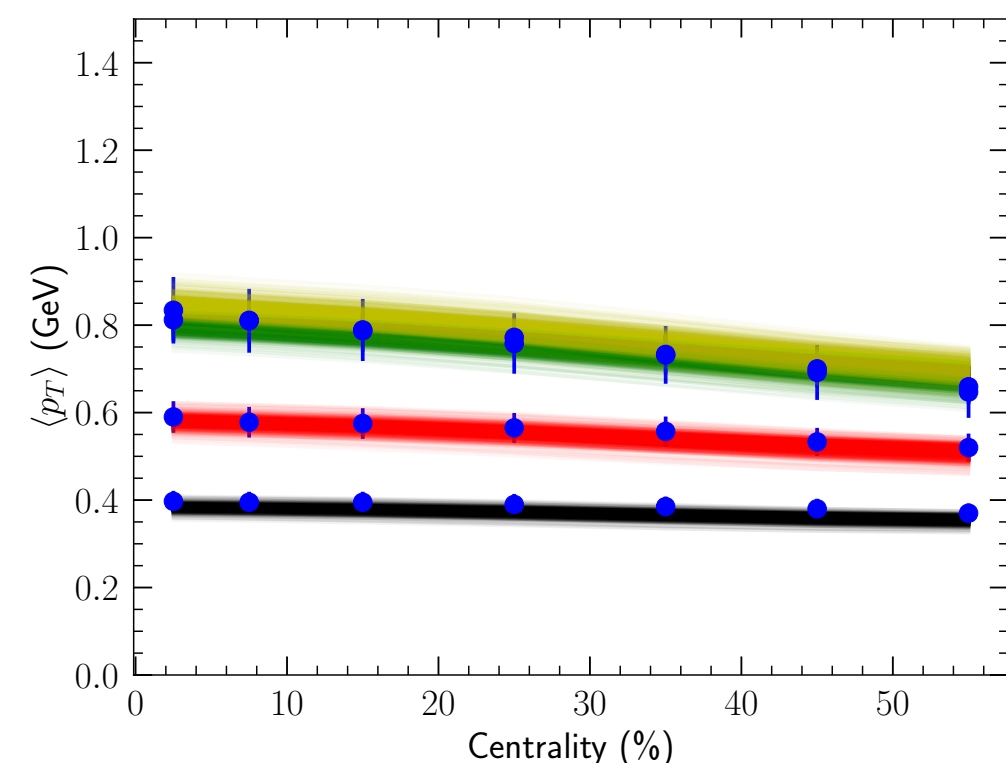
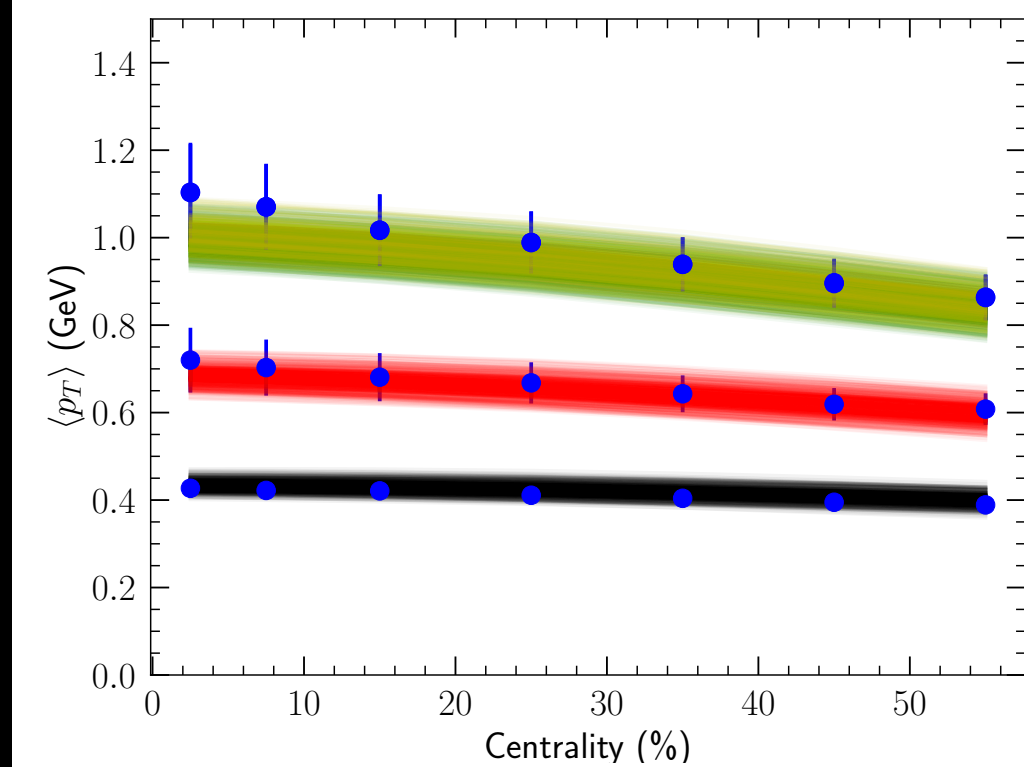
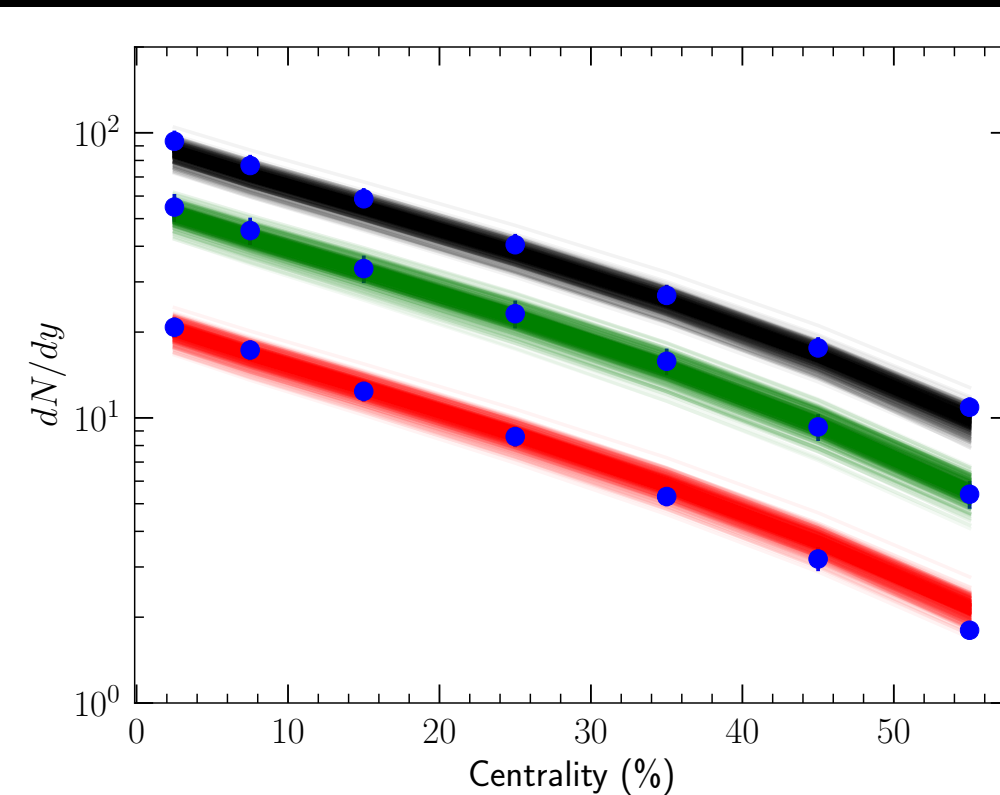
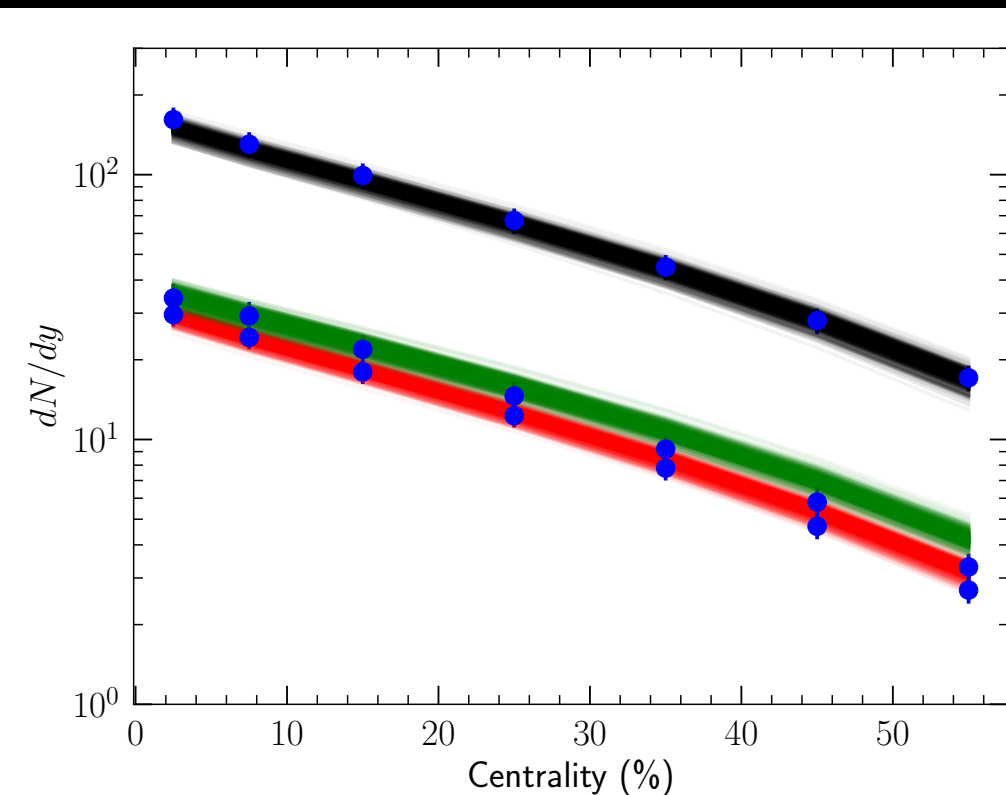
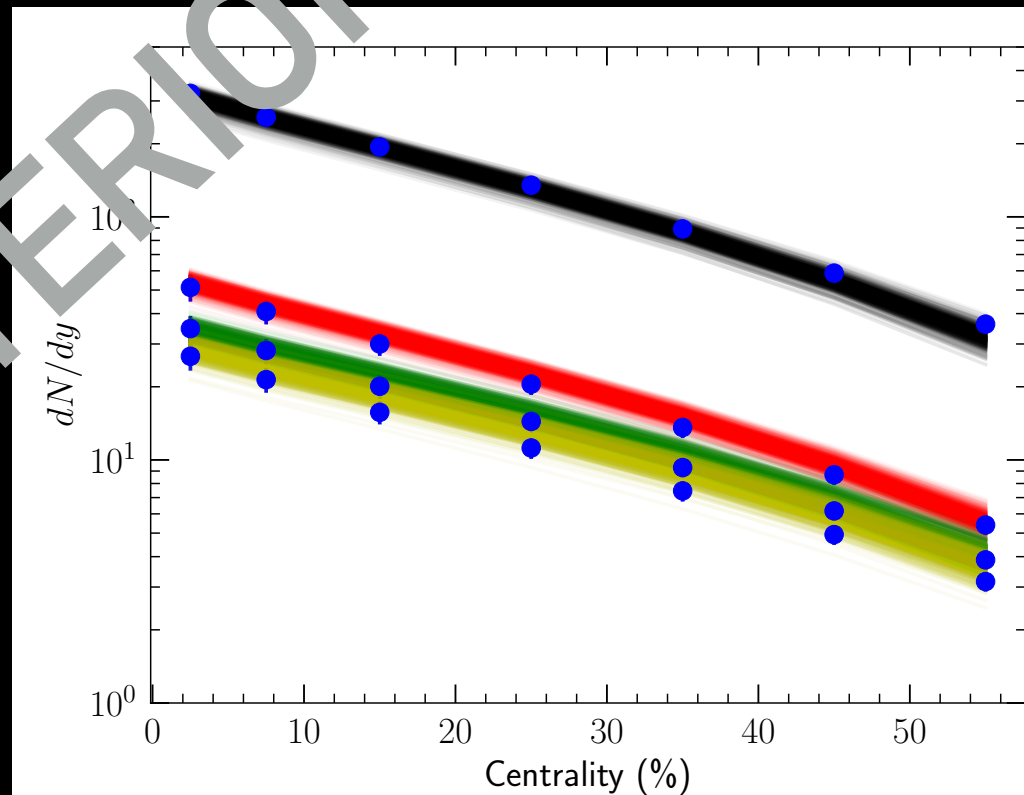
STAR



PHOBOS

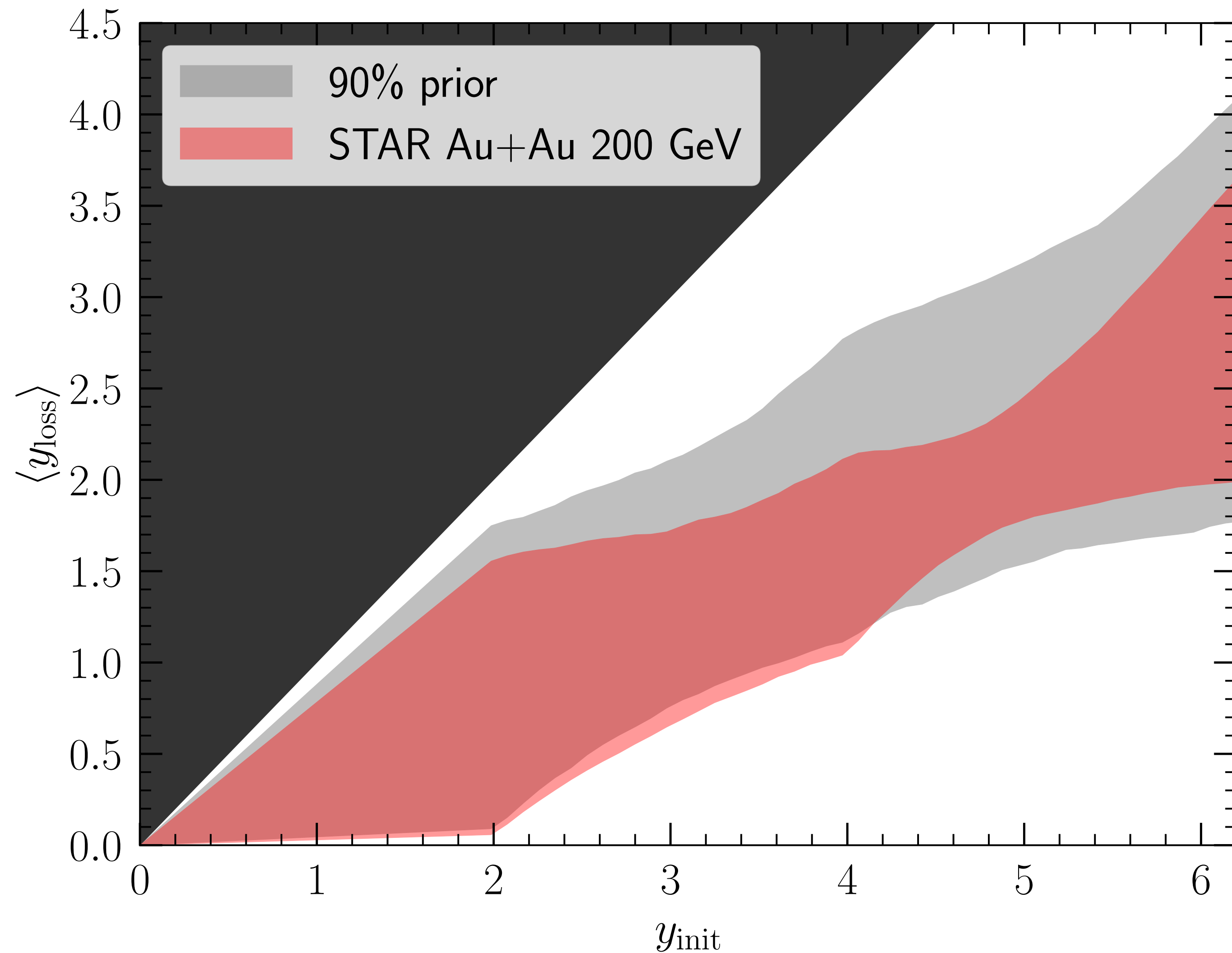
BAYESIAN INFERENCE AT RHIC BES ENERGIES

STAR



PHOBOS

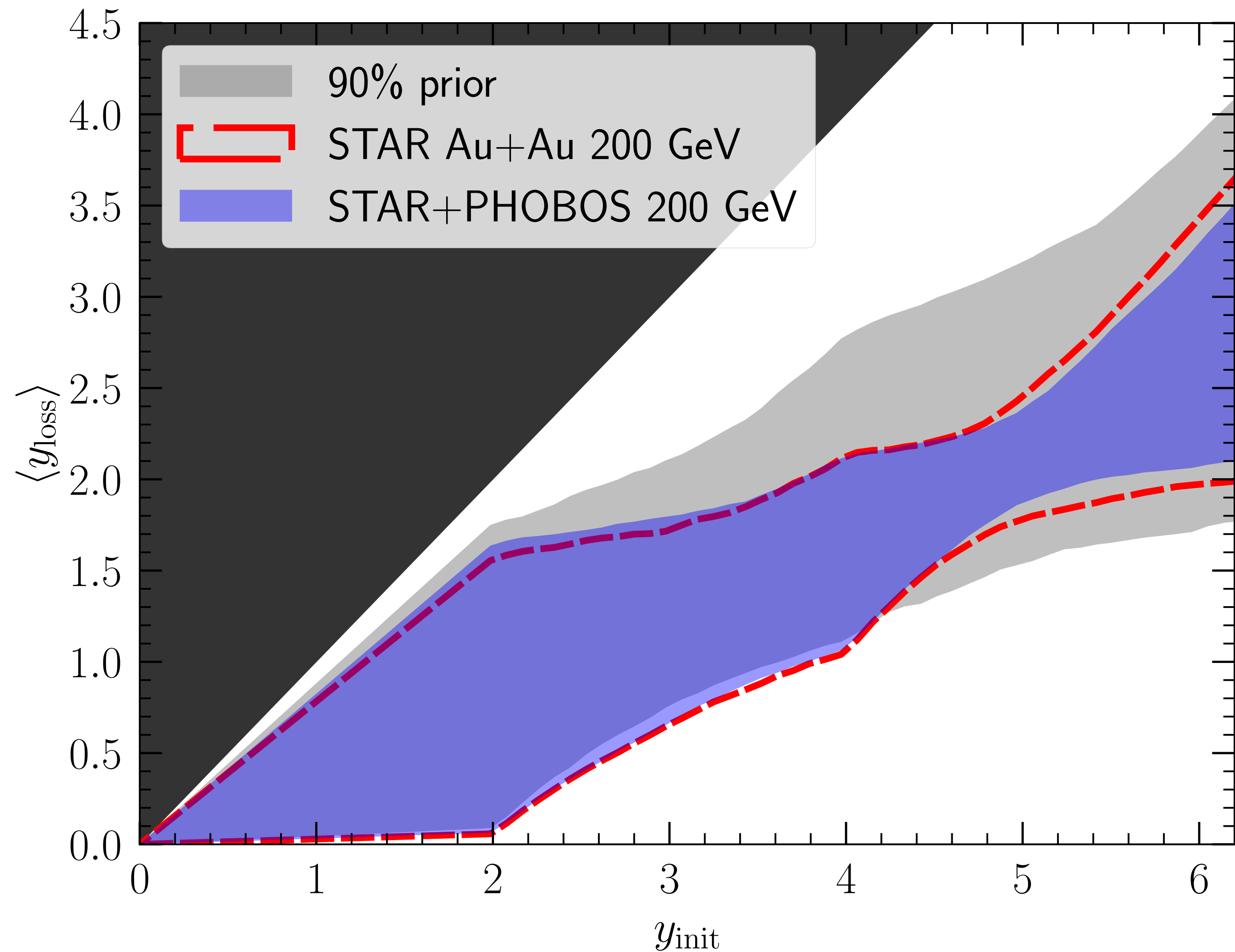
INITIAL-STATE STOPPING



- Mid-rapidity particle productions at 200 GeV yields $y_{\text{loss}} \sim 2$ for $y_{\text{init}} \sim 5$

color bands indicate 90% credible interval in the posterior

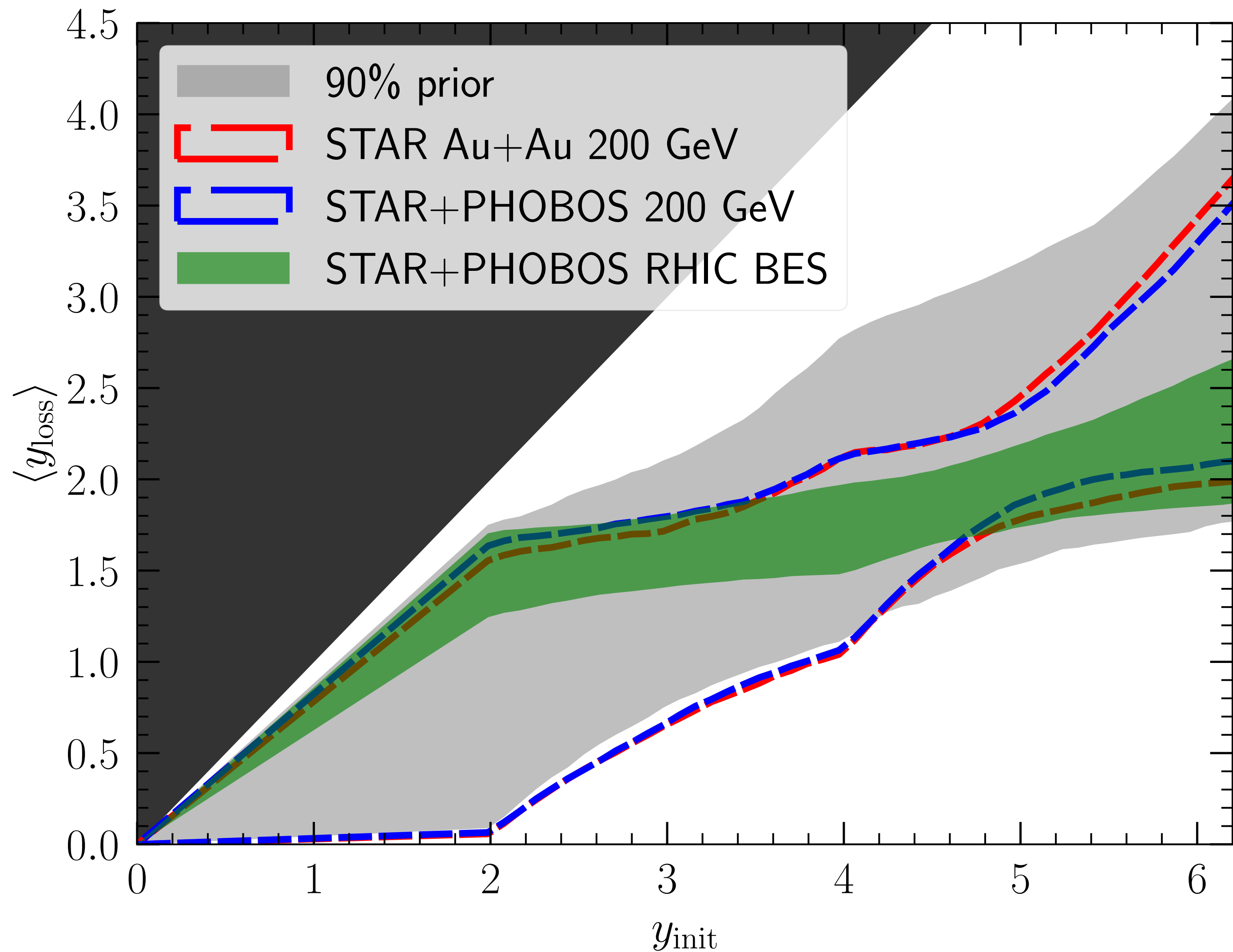
INITIAL-STATE STOPPING



- Mid-rapidity particle productions at 200 GeV yields $y_{\text{loss}} \sim 2$ for $y_{\text{init}} \sim 5$
- The rapidity distributions from PHOBOS give small improvements to the constraint

color bands indicate 90% credible interval in the posterior

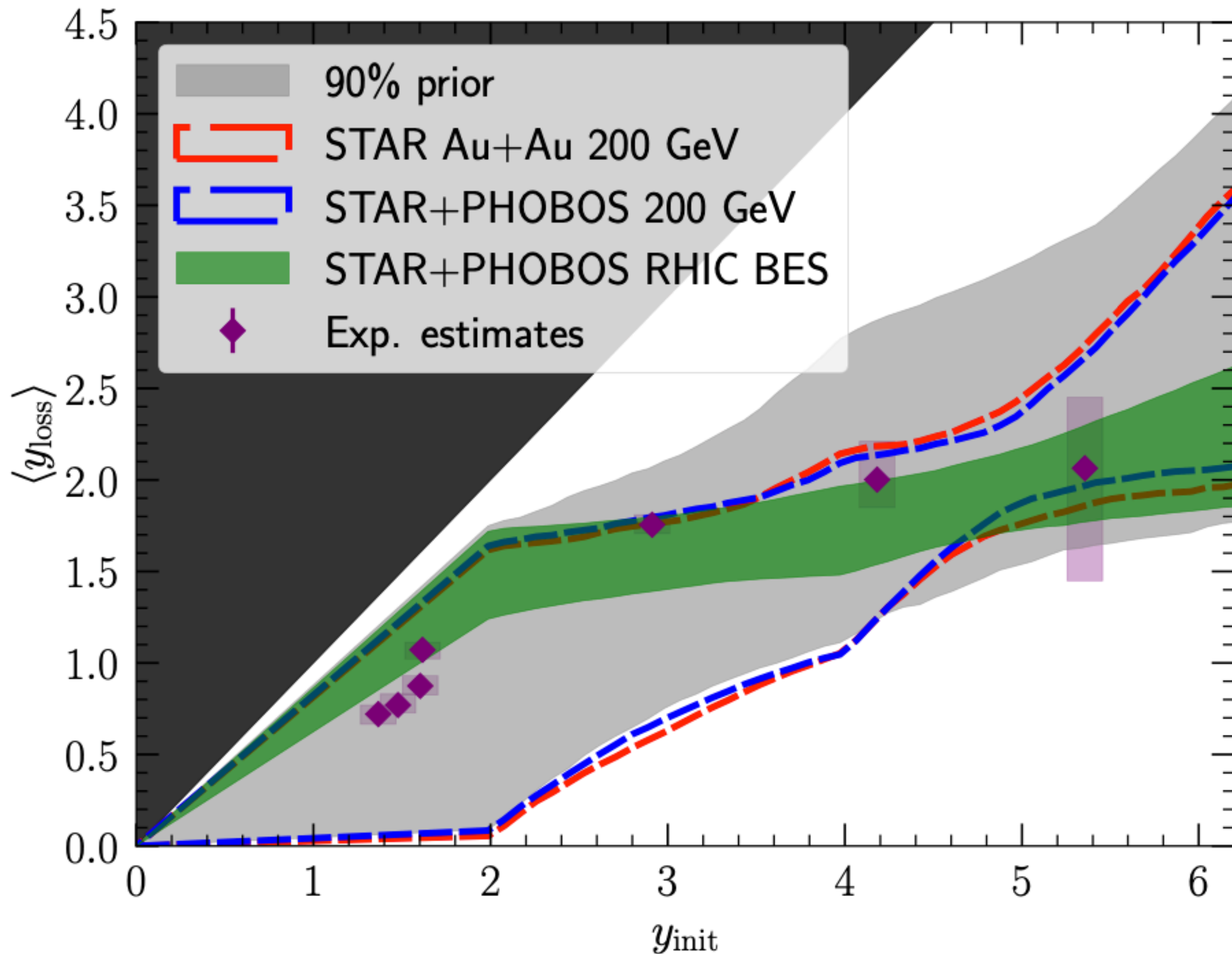
INITIAL-STATE STOPPING



- Mid-rapidity particle productions at 200 GeV yields $y_{\text{loss}} \sim 2$ for $y_{\text{init}} \sim 5$
- The rapidity distributions from PHOBOS give small improvements to the constraint
- Particle production from 7.7, 19.6, and 200 GeV sets **strong** constrain on $y_{\text{loss}}(y_{\text{init}})$ for $y_{\text{init}} \in [0,6]$

color bands indicate 90%
credible interval in the posterior

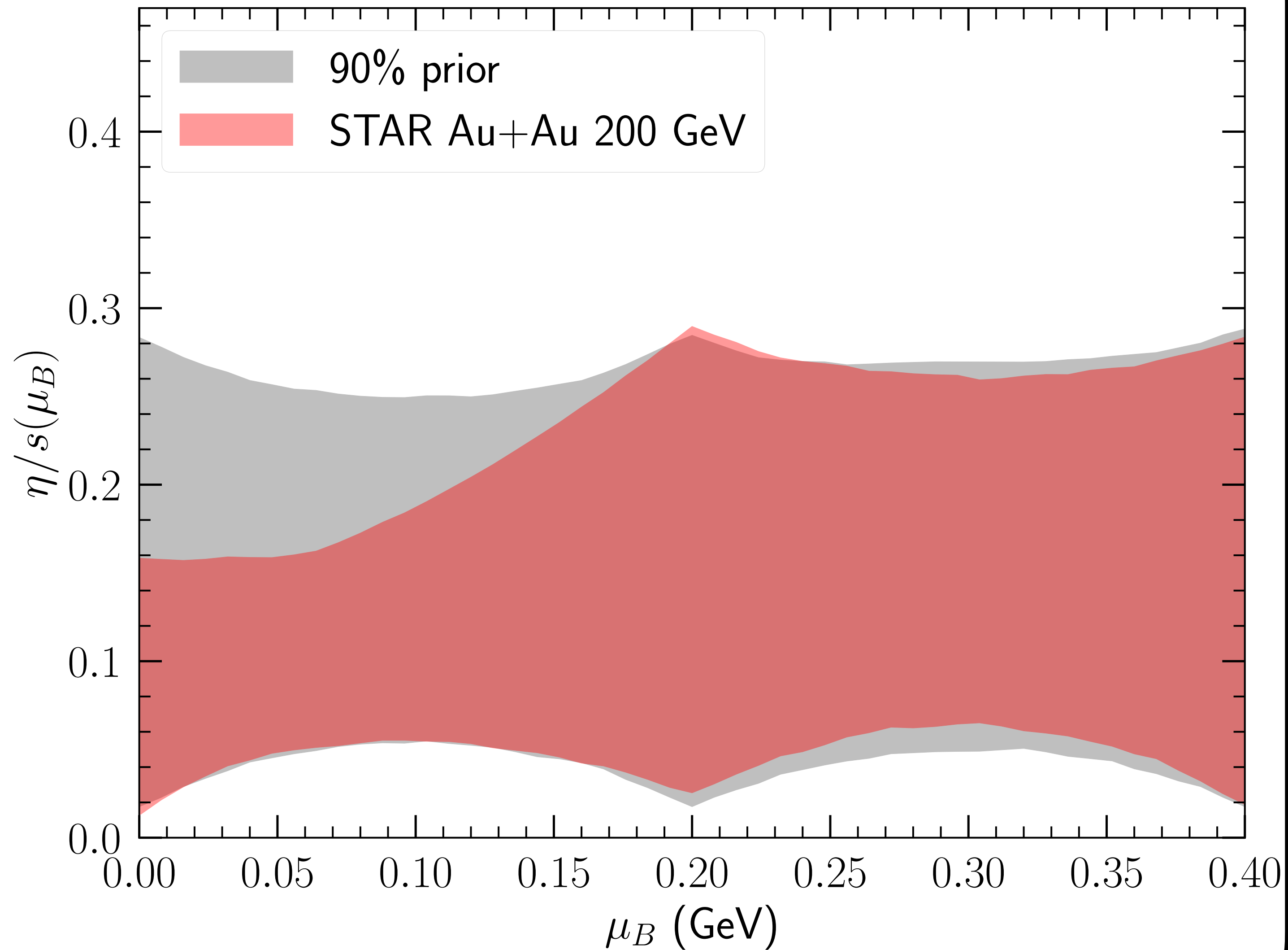
INITIAL-STATE STOPPING



- Mid-rapidity particle productions at 200 GeV yields $y_{\text{loss}} \sim 2$ for $y_{\text{init}} \sim 5$
- The rapidity distributions from PHOBOS give small improvements to the constraint
- Particle production from 7.7, 19.6, and 200 GeV sets **strong** constrain on $y_{\text{loss}}(y_{\text{init}})$ for $y_{\text{init}} \in [0,6]$

color bands indicate 90% credible interval in the posterior

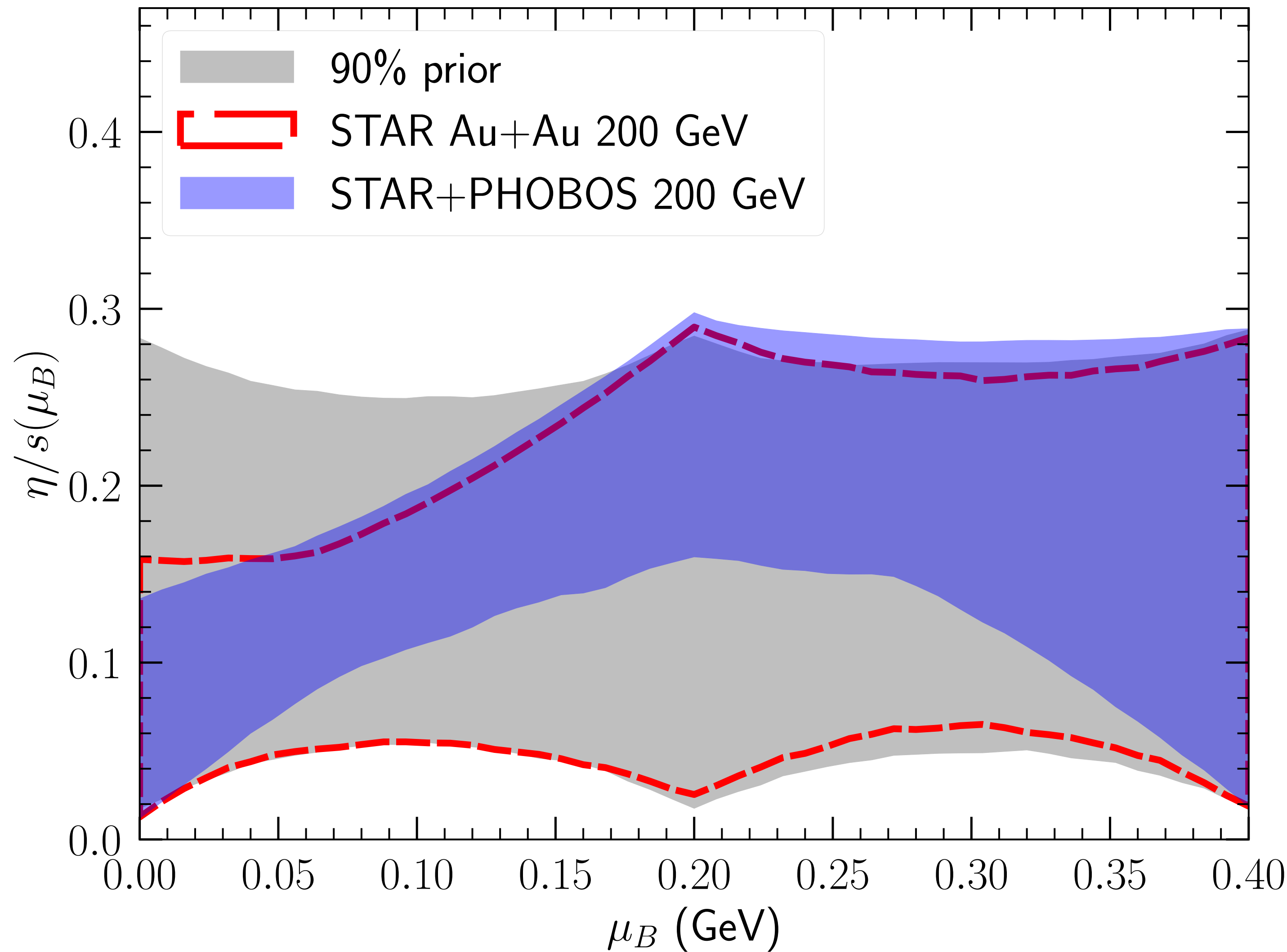
SHEAR VISCOSITY $\eta/s(\mu_B)$



- Mid-rapidity data at 200 GeV can constrain η/s around $\mu_B = 0$

color bands indicate 90% credible interval in the posterior

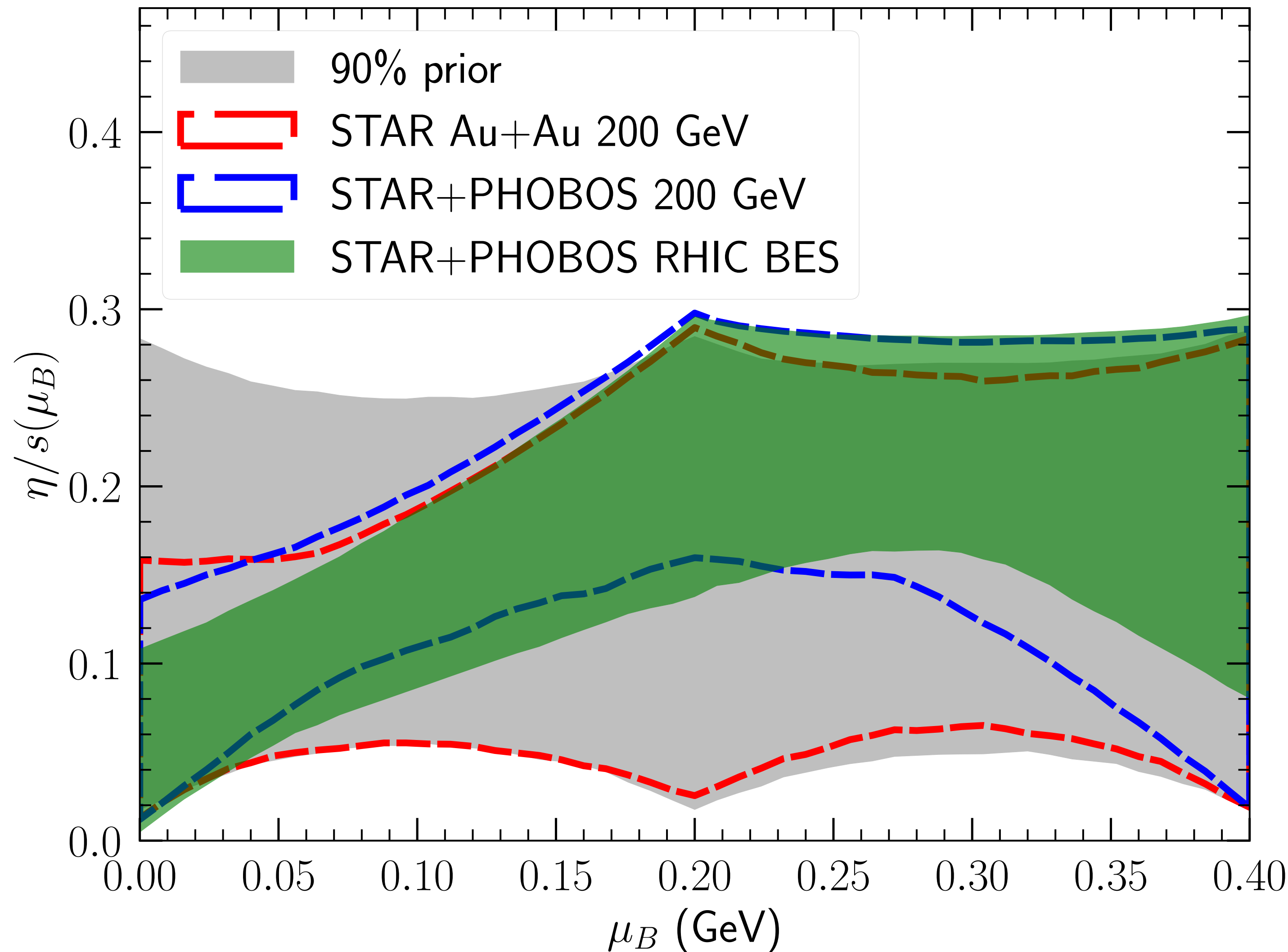
SHEAR VISCOSITY $\eta/s(\mu_B)$



- Mid-rapidity data at 200 GeV can constrain η/s around $\mu_B = 0$
- The $dN^{\text{ch}}/d\eta$ and $v_2(\eta)$ at 200 GeV significantly improve the η/s constraint at $\mu_B \sim 0.2$ GeV

color bands indicate 90% credible interval in the posterior

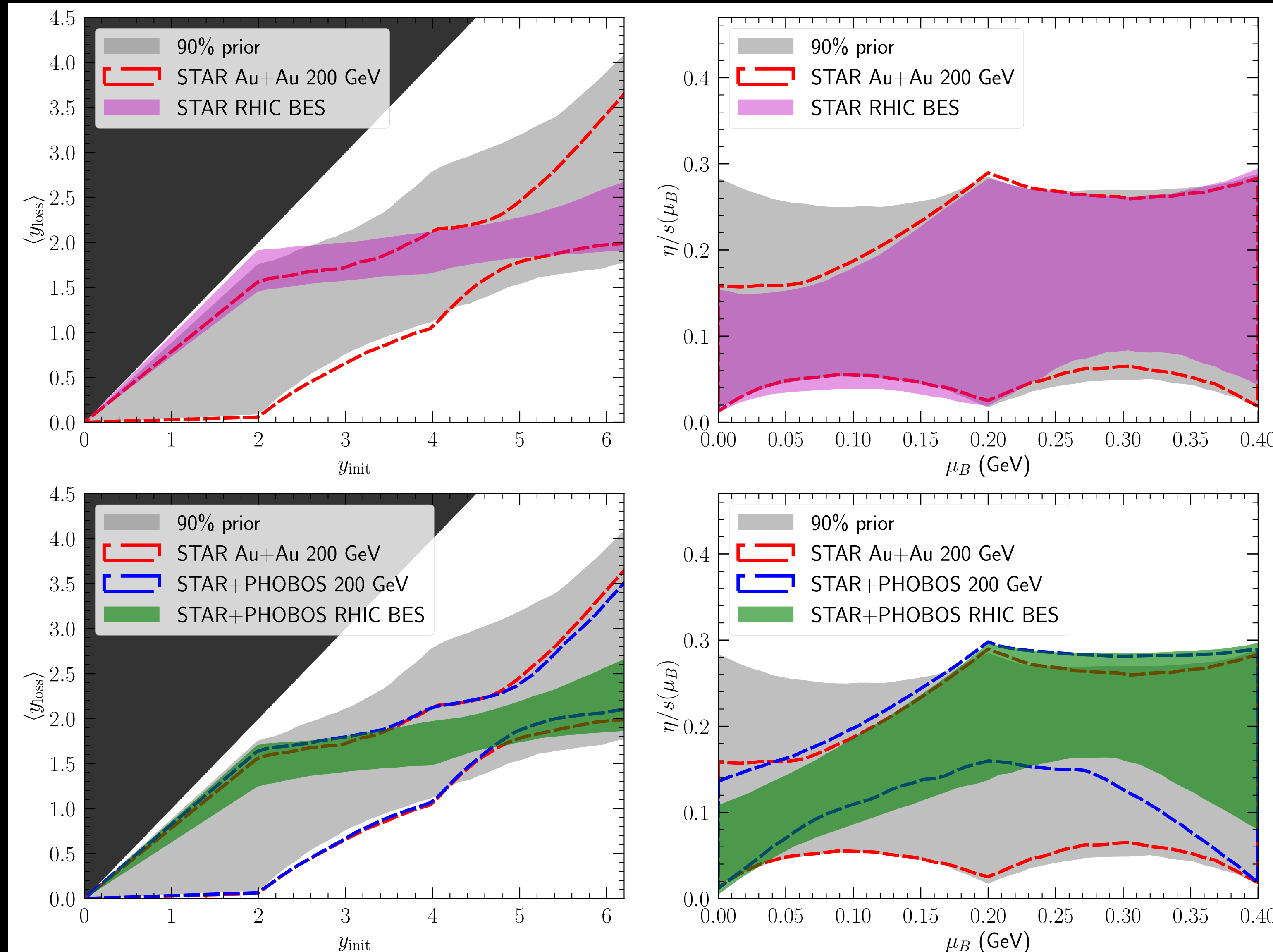
SHEAR VISCOSITY $\eta/s(\mu_B)$



- Mid-rapidity data at 200 GeV can constrain η/s around $\mu_B = 0$
- The $dN^{\text{ch}}/d\eta$ and $v_2(\eta)$ at 200 GeV significantly improve the η/s constraint at $\mu_B \sim 0.2$ GeV
- The full RHIC BES data (STAR+PHOBOS) shows that the QGP η/s is **larger** at finite μ_B than that at $\mu_B = 0$

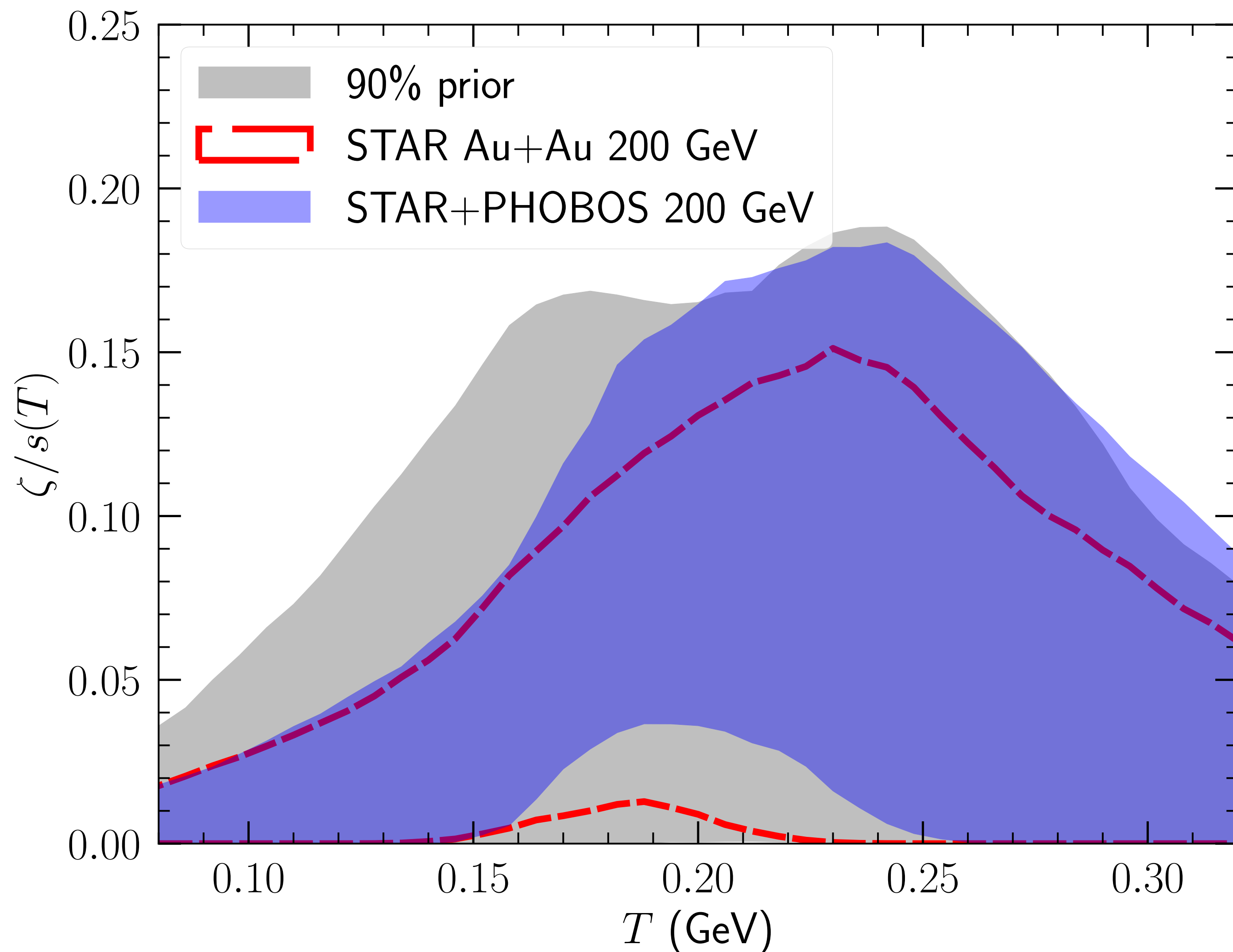
color bands indicate 90% credible interval in the posterior

INFERENCE WITH ONLY STAR MID-RAPIDITY DATA



- The mid-rapidity data from STAR BES energies can set a good constraint on $y_{\text{loss}}(y_{\text{init}})$
- The rapidity dependent $v_2(\eta)$ measurement imposes strong constraints on $\eta/s(\mu_B)$

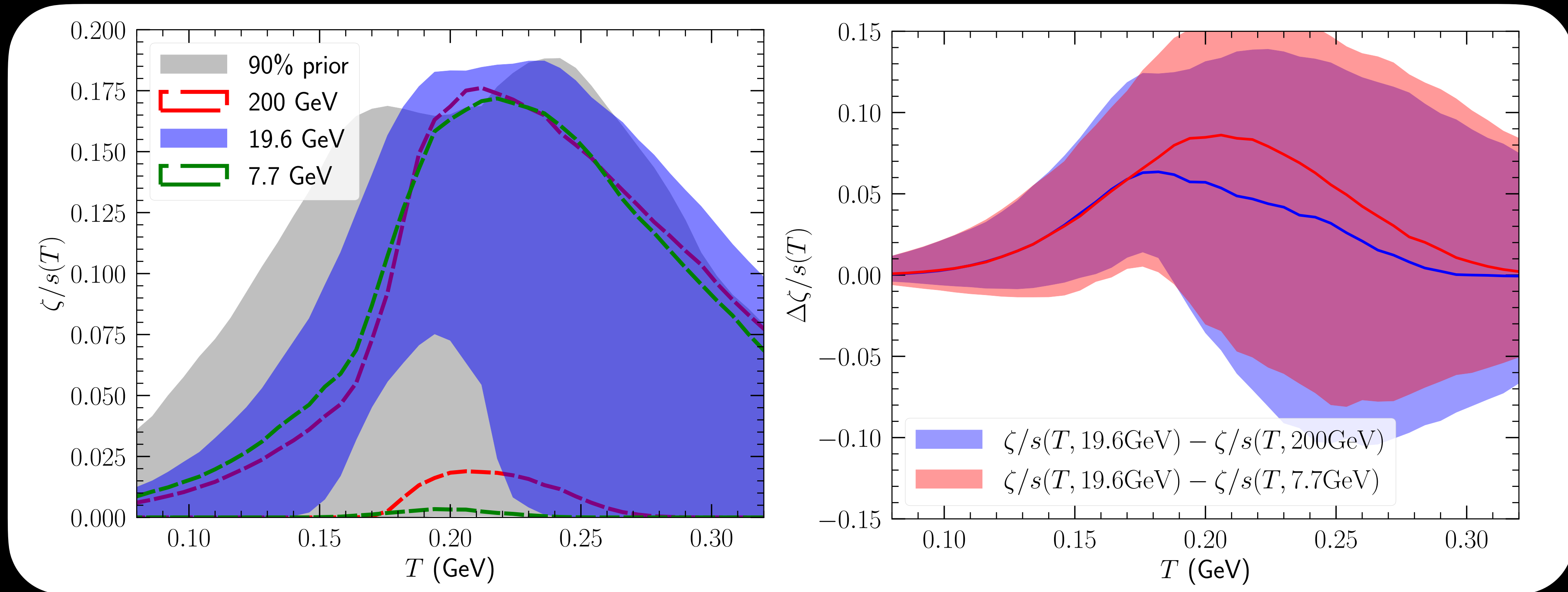
BULK VISCOSITY $\zeta/s(T)$



- Mid-rapidity identified particle yields and their $\langle p_T \rangle$ at 200 GeV set constraints on the temperature dependence of the QGP bulk viscosity
- The additional PHOBOS data shifts the posterior $\zeta/s(T)$ to larger values

color bands indicate 90% credible interval in the posterior

BULK VISCOSITY $\zeta/s(T, \sqrt{s})$

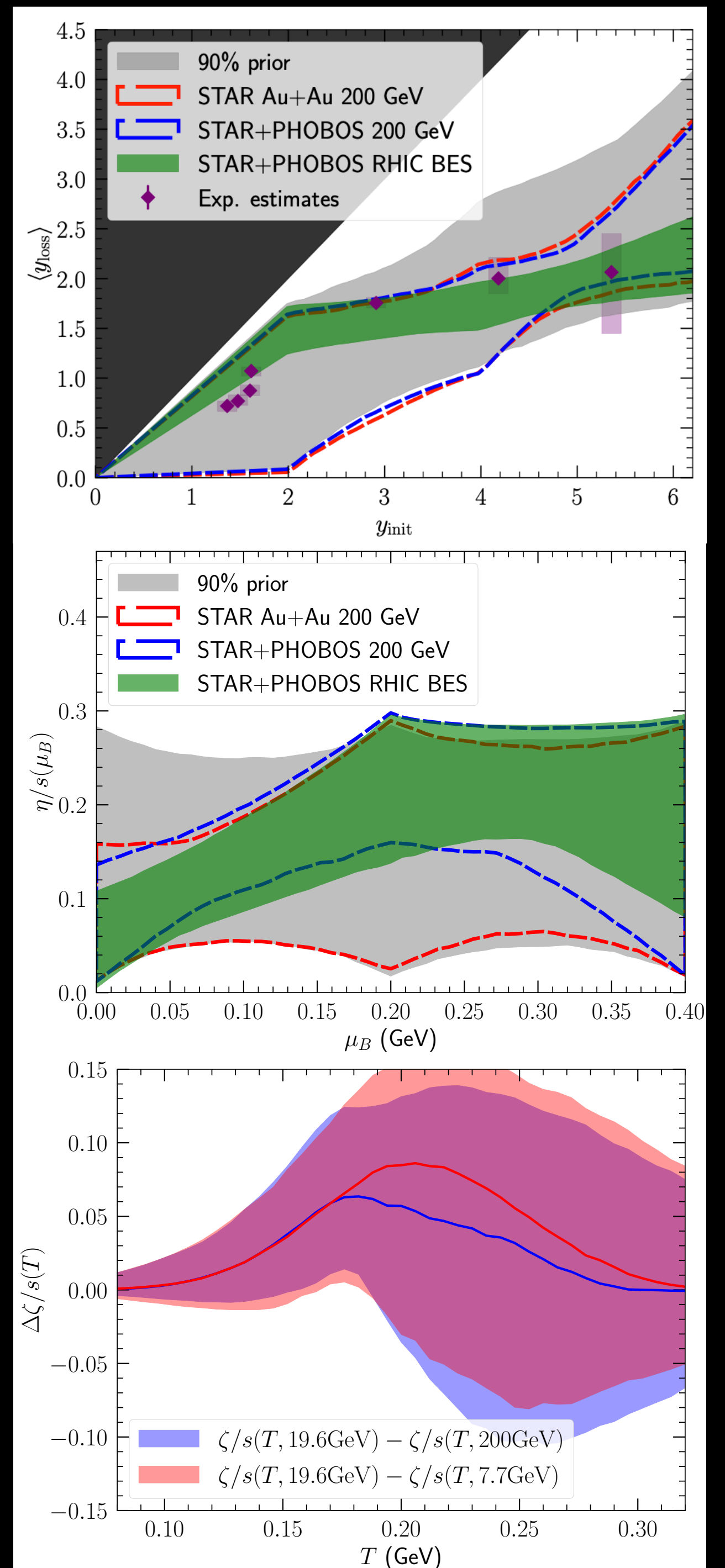


- Allowing $\zeta/s(T)$ to be an independent function for the three collision energies, our calibration suggests a **larger** $\zeta/s(T)$ at 19.6 GeV than those at 200 and 7.7 GeV for $T \in [0.15, 0.2]$ GeV

Hint for softening(hardening) EoS at $\mu_B = 0.2(0.4)$ GeV?

CONCLUSIONS

- We performed a comprehensive Bayesian Inference study at multiple RHIC BES energies with a state-of-the-art event-by-event (3+1)D hybrid framework
- With the RHIC BES phase I data, **robust constraints** are obtained for initial state nuclear stopping, QGP $\eta/s(\mu_B)$, and $\zeta/s(T, \sqrt{s})$ for the first time
- The QGP effective η/s is larger at finite μ_B , while $\zeta/s(T)$ shows a hint for **non-monotonic** energy dependence around $\sqrt{s} = 19.6$ GeV
- Our work marks an important step towards **quantitative characterization** of the QCD phase structure with the RHIC BES and future FAIR programs



OUTLOOK

- Confront with the RHIC BES phase II data
 - ➔ Constrain the speed of sound $c_s^2(T, \mu_B)$
 - ➔ Extend to multiple conserved charge currents $P(e, n_B, n_Q, n_S)$
 - ➔ Critical fluctuations/first-order phase transition
- (3+1)D dynamics at the LHC
 - ➔ Rapidity (small-x) evolution
 - ➔ The role of nuclear structure
- Open data
 - ➔ Engage more collaboration on developing robust and efficient statistical analyses